SUBGRADE STRAINS MEASURED IN FULL-SCALE TRAFFIC TESTS WITH FOUR- AND SIX-WHEEL LANDING GEARS

By:
Gordon F. Hayhoe
FAA William J. Hughes Technical Center
Airport Technology Research and Development Branch, AAR-410
Atlantic City International Airport, NJ 08405, U.S.A.
Phone: (609) 485- 8555; FAX: (609) 485-4845
gordon.hayhoe@tc.faa.gov

and

Navneet Garg
Galaxy Scientific Corporation
2500 English Creek Ave., Bldg. C
Egg Harbor Twp., NJ 08234-5562, U.S.A.
Phone: (609) 645-0900; FAX: (609) 645-2881
navneet.garg@galaxyscientific.com

PRESENTED FOR THE 2002 FEDERAL AVIATION ADMINISTRATION AIRPORT TECHNOLOGY TRANSFER CONFERENCE

05/02

ABSTRACT

Vertical strains were measured in the subgrade of a conventional flexible airport pavement test item during full-scale traffic tests at the National Airport Pavement Test Facility. The tests were run to complete failure over approximately 12,000 repetitions. Load was applied in separate wheel paths by landing gear configurations representative of typical four- and six-wheel jet transport aircraft landing gears. Wheel load was 45,000 pounds on both gears over the complete test. The wander path was 2 meters (6.5 ft) wide with 66 repetitions in a complete wander cycle. Multidepth deflectometers (MDDs) were located at a single lateral position relative to the center of the wander pattern in each wheel path. Average strains in the top 150 mm (6 in) of the subgrade were computed from subgrade deflections measured with the MDDs. Representative time histories of the strains are shown to illustrate the response behavior at different lateral positions of the gear in a wander cycle and at different times in the test from the start of the test to complete failure. The relationship between recovered and unrecovered strains at different positions in the wander cycle is also illustrated by the time histories. Over a complete wander cycle, unrecovered strains vary from large compressive to large expansive relative to the mean value. Net unrecovered strain over a complete wander cycle is very small both in absolute terms and relative to the unrecovered strains at individual wander positions. The net unrecovered strain over a single wander cycle represents the permanent deformation in the subgrade accumulated over that wander cycle. When accumulated over the complete test to failure, these small increments of permanent deformation represent the contribution of the subgrade to total rut accumulation. Both the recovered strains and the unrecovered strains increased in magnitude as testing progressed to failure. Also, the ratio of unrecovered strain to recovered strain increased as testing progressed. Summaries are given of the recovered and unrecovered vertical strains for six complete wander cycles at different times as the test progressed from start to end. Summaries are also given of the recovered and unrecovered strains at one wander position over many wander cycles to show the relationship between maximum strain and load repetitions. The strain measurements demonstrate that the response of the pavement is extremely complex and that realistic theoretical modeling of the pavement structure requires a model which includes permanent deformation, moving loads with wander, repeated loading, and representation of structural parameters as functions of temperature and accumulation of damage.

INTRODUCTION

The first flexible pavement test item to fail at the Federal Aviation Administration's (FAA) National Airport Pavement Test Facility (NAPTF) was the medium-strength subgrade conventional pavement designated MFC. The structure consisted of 5 in of dense graded asphaltic concrete meeting the FAA specification P-401, 8 in of P-209 crushed aggregate base course, and 12 in of P-154 subbase course placed on a clay subgrade having a nominal (target) California Bearing Ratio (CBR) of 8 percent, as shown in figure 1. (See reference 1 for the FAA material specifications. Also see the AAR-410 website, http://airporttech.tc.faa.gov, for measured properties of the materials used in the construction.) Six-wheel traffic was applied to the north wheel track and four-wheel traffic was applied to the south wheel track. The test item was 18.3 m (60 feet) wide and 19 m (62.5 feet) long. The condition of the pavement structure was monitored during the tests by measuring the surface properties (rut depth, transverse profiles, and cracking). These measurements were used to determine when failure had occurred.

However, other measurements were made of the structural response of the pavement during the tests. Of particular interest in the manner of the failure of the pavement is the strain in the subgrade material at, or close to, the top of the subgrade. The purpose of this paper is to present and discuss measurements made of the average vertical strain within approximately the top 150 mm (6 in) of the subgrade. The general test conditions are described first.

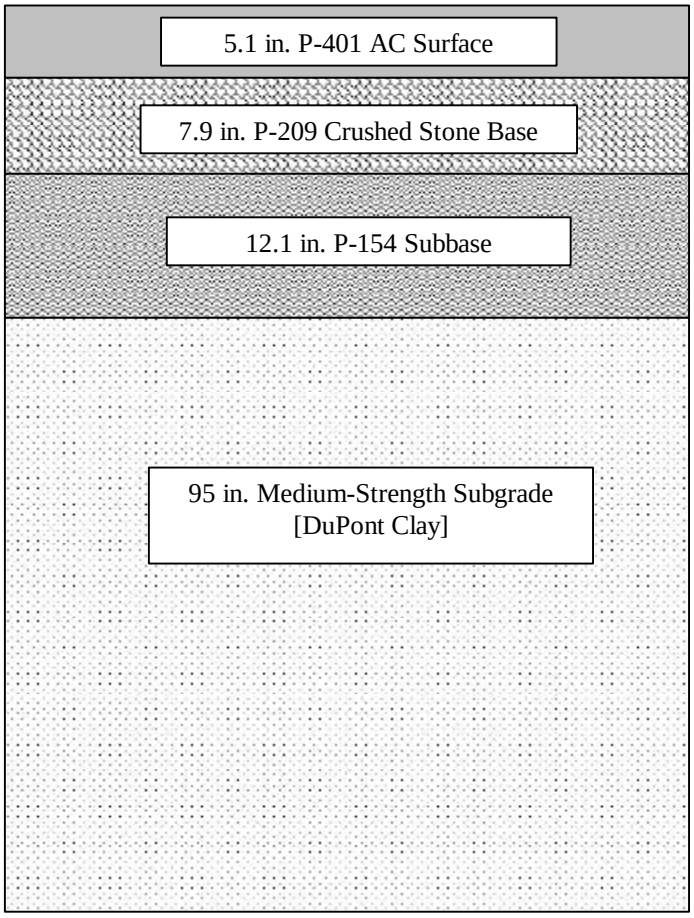

Figure 1. Cross-sectional details of test item MFC. Dimensions are as reported in the as-built drawings. Nominal thicknesses were 5 in (127 mm), 8 in (203 mm), and 12 in (305 mm).

Failure Criterion. The objective of the tests was to determine the amount of traffic required to cause shear failure in the subgrade. The failure criterion was the presence of at least 25.4 mm (1 inch) of surface upheaval adjacent to the traffic lane. This is the same as the criterion used by the U.S. Army Corps of Engineers in previous full-scale tests of flexible airport pavements (see, for example, reference 2). Failure in both wheel tracks occurred at approximately 12,000 repetitions, with maximum rut depth of 4 in and maximum upheaval of 1.5 in, both measured relative to the original grade. A trench was opened across the full width of the test item after trafficking was completed to measure the material properties of the structure and the profiles of the interfaces between the different layers. Profile measurements from the trenching confirmed that shear failure had occurred in the subgrade, see reference 3.

Rut Depth Measurements. Transverse profile measurements were made throughout trafficking as were rut depth measurements. The rut depths were measured with a 3.66 m- (12

foot-) long straightedge. These measurements were made at intervals of approximately 350 load repetitions to track the structural deterioration of the test item and to determine when the failure criterion had been satisfied.

Multidepth Deflectometer Measurements. Additional measurements of structural response included high-speed recording of vertical deflections from four multidepth deflectometers (MDDs) located in the wheel paths. Figure 2 shows the horizontal locations of the MDDs within the test item. Traffic paths 1 and 2 are 4.57 m (15 feet) to the north and south of centerline of the test pavement, respectively. (Note: they are not in the centers of the traffic wheel paths, as discussed below.) The MDDs each contain seven sensors which measure the vertical displacement of the structure at seven levels relative to the surface layer as shown in figure 3. The deflection relative to the lowest (anchor) level is calculated by subtracting the deflection of the level of interest from the deflection of the anchor sensor. Absolute deflections are not presented in this paper, only relative deflections in the subgrade. Data was collected from the MDD sensors at a rate of 20 times per second.

Traffic Loading and Wander. The north wheel track was loaded with a six-wheel dual-tridem gear configuration having 1,372-mm (54-inch) dual spacing and 1,448-mm (57-inch) tandem spacing. The south wheel track was loaded with a four-wheel dual-tandem gear configuration having 1,118-mm (44-inch) dual spacing and 1,473-mm (58-inch) tandem spacing. Wheel loads were set at 20.4 tonnes (45,000 lbs) each throughout the tests. This gives “strut” loads of 122.4 tonnes (270,000 lbs) on the six-wheel side and 81.6 tonnes (180,000 lbs) on the four-wheel side. Traffic speed was 8 km/h (5 mph).

A fixed wander pattern was applied to the traffic during the tests. The wander pattern consisted of 66 repetitions, 33 traveling east and 33 traveling west. The transverse position of the gears was changed only at the start of the eastward repetitions. That is, westward repetitions always had the wheels following in the same paths as in the preceding eastward repetition. The wander pattern was designed to simulate a normal distribution with standard deviation of 775 mm (30.5 in) (equivalent to a taxiway distribution for design). The distribution of the transverse wheel positions is not random, but consists of nine equally spaced wheel paths at intervals of 260 mm (10.25 in). The pattern is similar to the patterns used in previous full-scale airport pavement traffic tests except that one wander cycle includes a larger number of repetitions than were typically used before (see reference 2). Figure 4 shows the wander distribution and table 1 shows the transverse positions of the gear centers for each wander position in the cycle. Note that the mean wander positions are not at the centers of the traffic paths (+/- 4.57 m (15 feet)) and are not at equal distances from the centers. This was caused by the need to position the wheels on the two gears at defined, and equal, transverse distances from the longitudinal joints of the rigid pavement test items also located in the test pavement. Figure 5 shows the transverse positions of the centers of the gears and wheels relative to the MDD locations for all nine wander positions. The figure shows, from top to bottom, the first 18 repetitions (9 wander positions) in the wander sequence. The gears move in phase, with both gears moving left and right together rather than towards and away from each other. This was done to minimize interaction of the gear loads at the subgrade level.

Data Availability. All data referenced in this paper will be available for public download on the FAA AAR-410 website www.airporttech.tc.faa.gov.

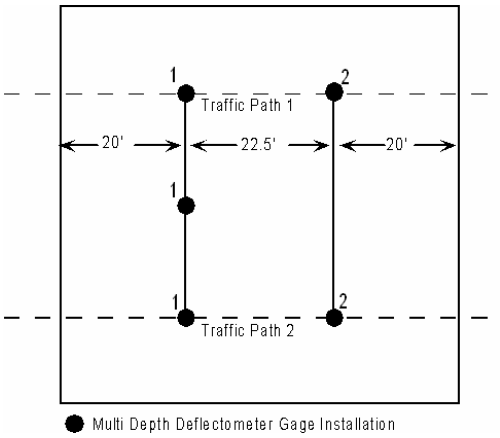

Figure 2. Horizontal locations of the multidepth deflectometers in test item MFC.

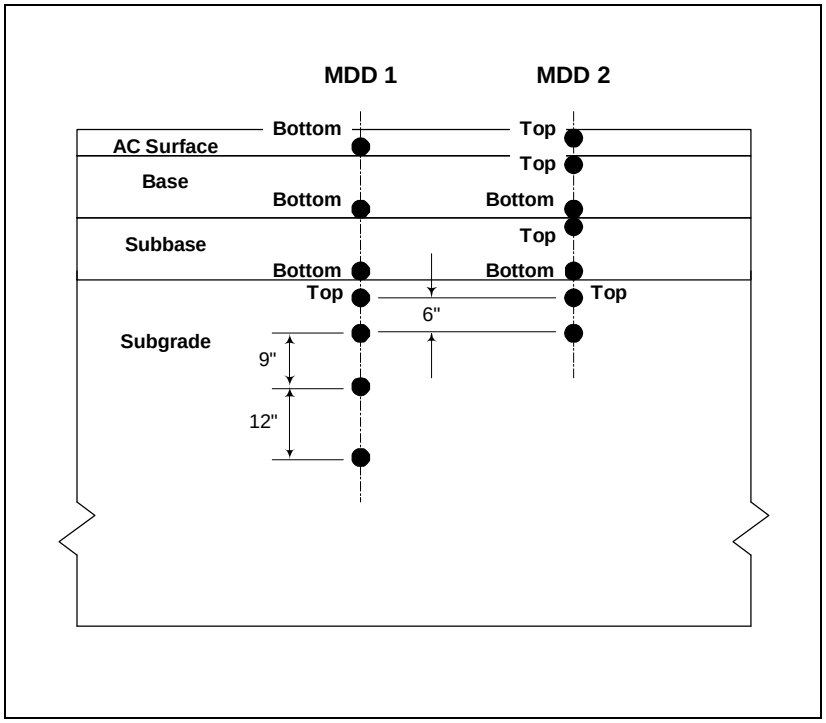

Figure 3. Vertical locations of the MDD sensors in test item MFC. The separation of the sensors across the subbase/subgrade interface is approximately 50 mm (2 in).

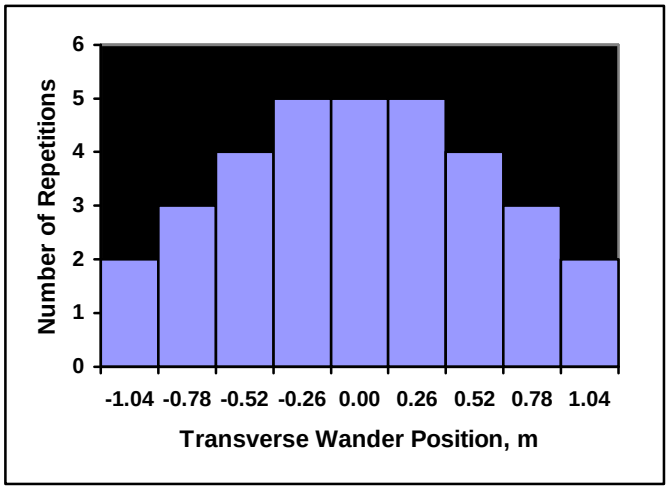

Figure 4. Histogram of the number of repetitions at each wander position in a complete wander cycle.

Table 1.
Transverse gear centerline (CL) positions in a complete wander cycle. Gear CL positions are defined as negative to the north of the test pavement CL and positive to the south. Travel direction is eastward for odd sequence numbers and westward for even sequence numbers.

Sequence No	Track No	North Gear CL Posn, m	South Gear CL Posn, m		Sequence No	Track No	North Gear CL Posn, m	South Gear CL Posn, m
1,2	-4	-4.939	2.719		35,36	-3	-4.679	2.979
3,4	-2	-4.419	3.239		37,38	3	-3.119	4.539
5,6	0	-3.899	3.759		39,40	1	-3.639	4.019
7,8	2	-3.379	4.279		41,42	-1	-4.159	3.499
9,10	4	-2.859	4.799		43,44	-3	-4.679	2.979
11,12	3	-3.119	4.539		45,46	-2	-4.419	3.239
13,14	1	-3.639	4.019		47,48	0	-3.899	3.759
15,16	-1	-4.159	3.499		49,50	2	-3.379	4.279
17,18	-3	-4.679	2.979		51,52	-2	-4.419	3.239
19,20	-4	-4.939	2.719		53,54	0	-3.899	3.759
21,22	-2	-4.419	3.239		55,56	2	-3.379	4.279
23,24	0	-3.899	3.759		57,58	1	-3.639	4.019
25,26	2	-3.379	4.279		59,60	-1	-4.159	3.499
27,28	4	-2.859	4.799		61,62	1	-3.639	4.019
29,30	3	-3.119	4.539		63,64	-1	-4.159	3.499
31,32	1	-3.639	4.019		65,66	0	-3.899	3.759
33,34	-1	-4.159	3.499					

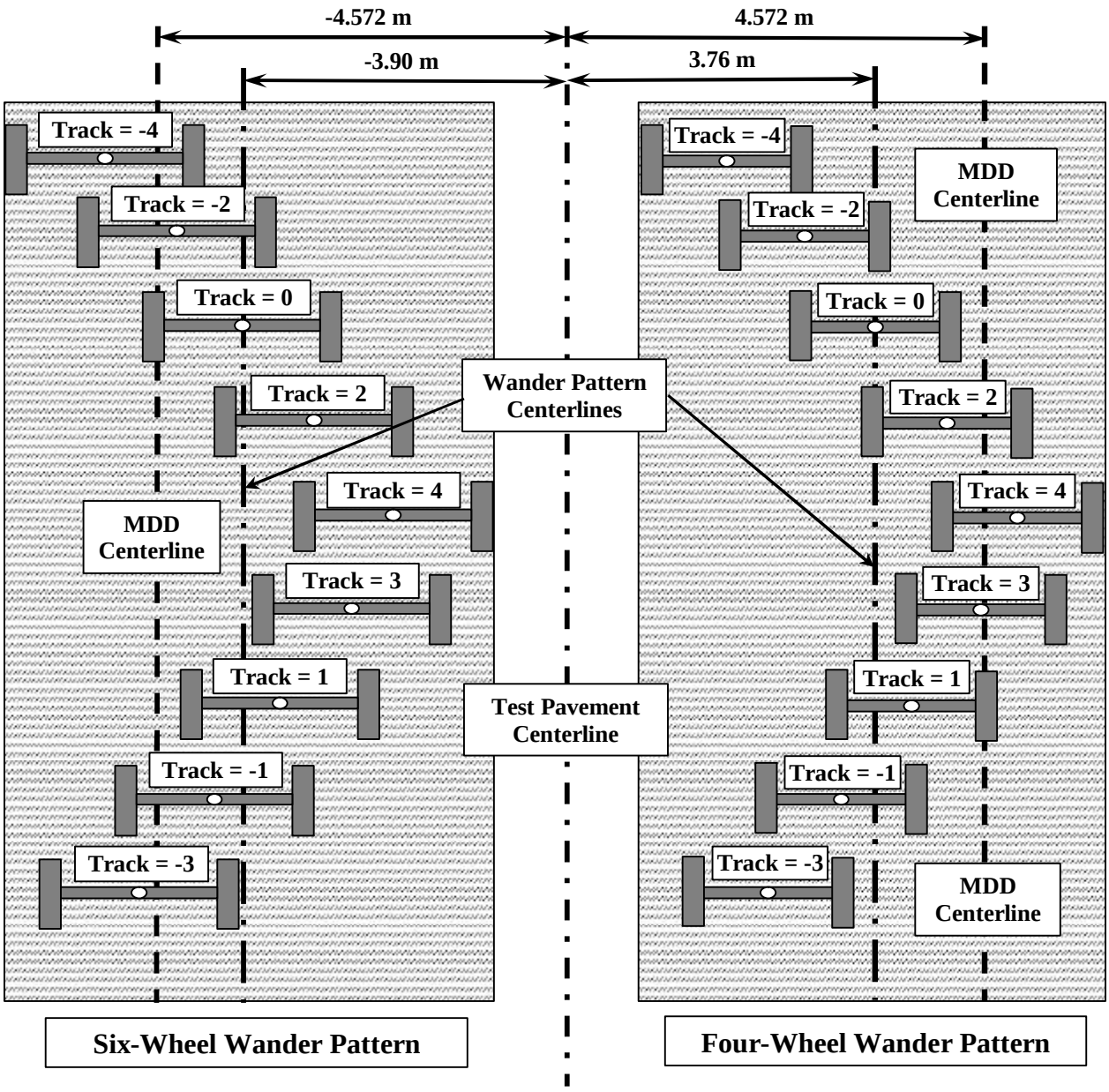

Figure 5. Six-wheel (north) and four-wheel (south) wander patterns showing the first nine positions relative to the MDD centerlines along the test item.

TYPICAL SUBGRADE STRAIN MEASUREMENTS

Subgrade strains are computed by measuring the deflection at two levels in the subgrade, subtracting one value from the other, and dividing by the distance between the sensors used to make the measurements. This gives, approximately, the average strain in the material separating the sensors. Figure 6 shows measurements of the difference between the two sensors in the top of the subgrade in MDD2 in the north traffic path of MFC, traffic path 1 in figure 2. The design condition was for the top sensor to be located 25 mm (1 inch) below the interface between the subbase and the subgrade and the lower sensor to be located 150 mm (6 in) below the top sensor.

Construction deviations from the design condition may have caused these dimensions to vary, particularly relative to the interface. It is also possible that the dimensions varied during the traffic tests.

Time histories are shown in the left column of figure 6 for travel in the east direction (after a change in the wander position) and in the right column for travel in the west direction (at the same wander position as in the previous pass in the east direction). The legend at the top of each time history gives the wander sequence number, the file name (including date), the sensor channel numbers, the measured value of relative deflection at the start of the time history (in inches), the end value minus the start value (in mils, 1 mil = 0.0254 mm), and the maximum negative-going value in the time history minus the end value (in mils). The last number in the legend therefore gives the recovered deflection between the sensors as the gear moves over the pavement in the vicinity of the MDD. The last but one number gives the unrecovered (permanent) deflection. Negative values denote a reduction in the distance between the sensors. The start and end values are computed as the averages of the first and last 20 samples, respectively. Strain is computed by dividing the recovered and unrecovered values by 6 (to give milli strain).

The time histories start at wander position 1 (sequence numbers 1 and 2) and end at wander position 9 (sequence numbers 17 and 18), corresponding to the gear and wheel positions shown in figure 5 from top to bottom. Notable features of the time histories are that.

- The largest recovered strain occurs when one of the tandem wheel groups passes directly over the MDD.
- Both positive (expansive) and negative (compressive) unrecovered strains occur, depending on the wander position. This behavior has been reported previously, as in, for example, references 4 and 5. Net accumulation of permanent deformation therefore occurs as a series of relatively large expansive and compressive deformations effectively canceling out over a single wander cycle. For example, the starting deformation value for the wander cycle in figure 6 is 0.1278 in (3.246 mm) and the final value is 0.1276 + 0.0007 = 0.1283 in (3.259 mm), an apparent (measured) expansion of 0.5 mils (0.013 mm). In contrast, the largest unrecovered strain for any repetition during the wander cycle is 5.2 mils (0.132 mm) between the start and end of wander sequence number 35.
- Unrecovered strains are typically larger in absolute magnitude when the gear is moving eastward than when it is moving westward (in the same wheel path as the eastward pass).
- Passage of the three axles is clearly defined by distinct peaks in the response when the wheels in one of the tandem groups are close to the MDD.
- The peak strain due to the wheels passing over the MDD increases significantly from the first wheel to pass over the MDD to the last wheel to pass over the MDD. This is in contrast to what would be expected in the response distribution for a nonmoving load or in the response distribution for an elastic pavement structure (whether the load is moving or not). In these two cases, the peak responses under the outer wheel loads would be equal and the peak response under the center wheel load would be somewhat higher.

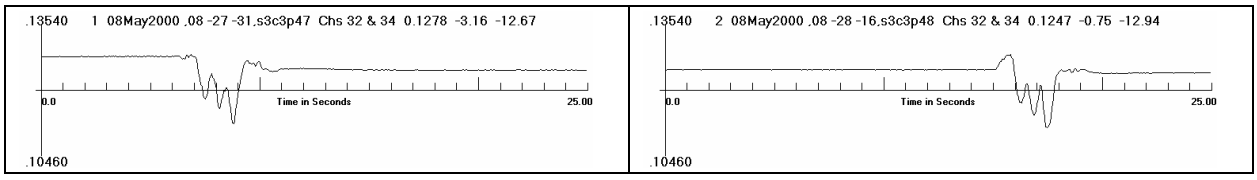

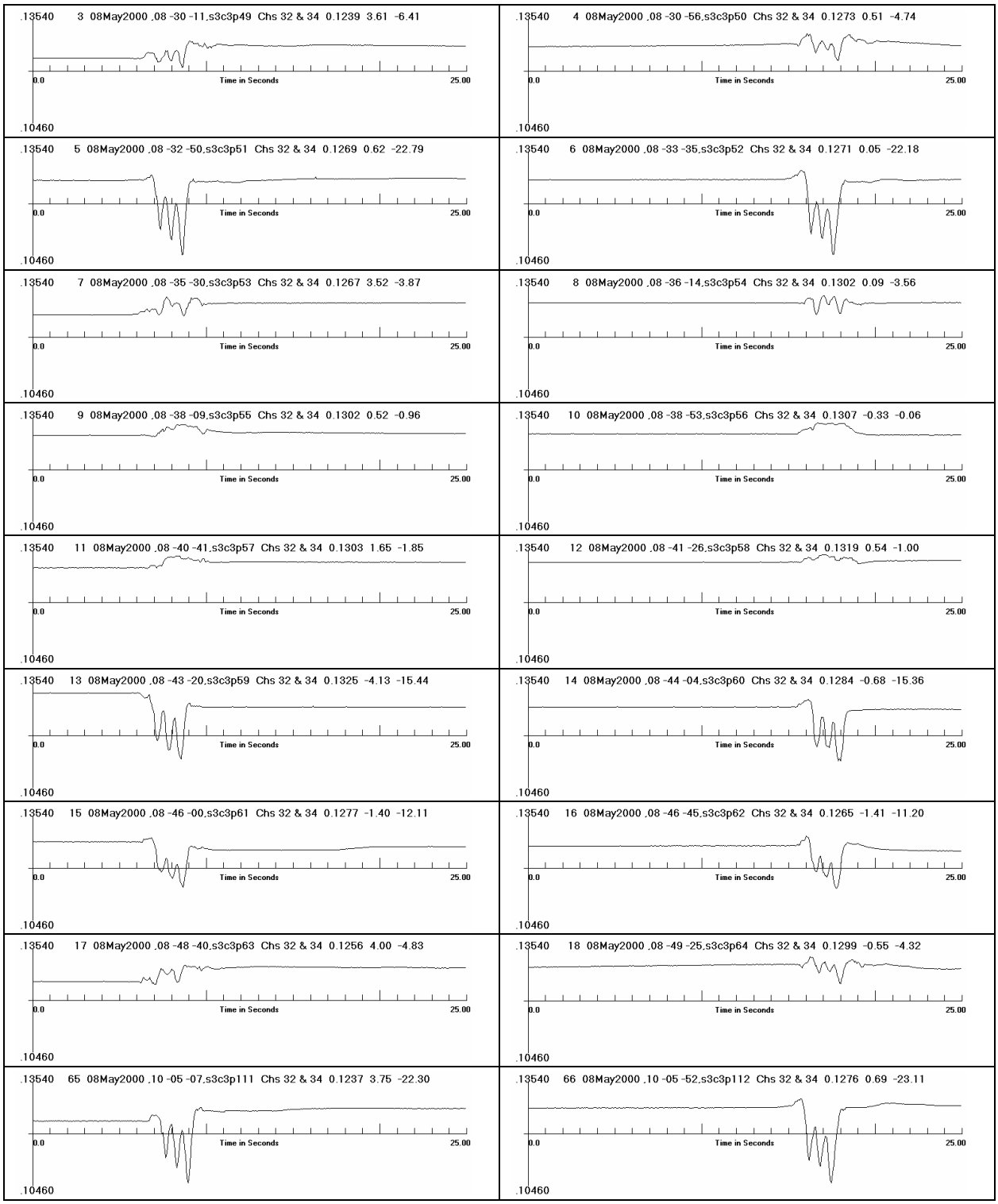

Figure 6. Time histories of relative displacement in the top 150 mm (6 in) of the subgrade under six-wheel loading. The left column is for the gear moving east and the right column is for the gear moving west. The last row gives the response at the last wander position (sequence numbers 65 and 66).

Figure 7 shows the response of the MDD2 sensors to the same passes of the test vehicle except under loading from the four-wheel gear. The characteristics of the response are the same as for loading under the six-wheel gear except that the unrecovered strains are significantly higher when the gear is moving eastward. When the gear is moving westward (in the same wheel path as the eastward pass), the unrecovered strains are very small. The maximum recovered strain, for the responses shown, again occurs when the wheels in a tandem group pass directly over the MDD, wander position 7, sequence numbers 13 and 14. The start position in this wander cycle is 0.0221 in (0.564 mm) and the end position is 0.0222 in, whereas the maximum unrecovered deflection is 13.9 mils (0.353 mm). This, together with the responses in figure 6, clearly demonstrates that, with wandered traffic, accumulation of permanent vertical deformation in the subgrade is not steady but occurs as a succession of compressive and expansive deflections. The compressive and expansive deflections are large compared to the net accumulated vertical deflection. When traffic is applied successively along the same path, as in the eastward-westward travel pairs illustrated in figures 6 and 7, the first pass can cause a large permanent deformation, with the magnitude depending on the position of the gear and the previous traffic history. Succeeding passes along the same path cause diminishing amounts of permanent deformation (at least for the structures and loads in the tests reported here). Pavement response to wandered traffic is therefore intrinsically different than for traffic applied only along one path. Reference 6 gives full-scale test data showing significantly lower life for wandered traffic than for traffic applied along only one path, presumably because of the different permanent deformation responses for the two types of traffic. One implication of this view of pavement response is that material properties measured in typical laboratory tests are not necessarily directly applicable to predictions of full-scale pavement life with wandered traffic.

Although response plots are not given, similar observations can be made about the responses of the unbound materials in the base and subbase materials as have been made about the subgrade responses (see figures 17 and 19 below for measured responses of the combined base and subbase layers).

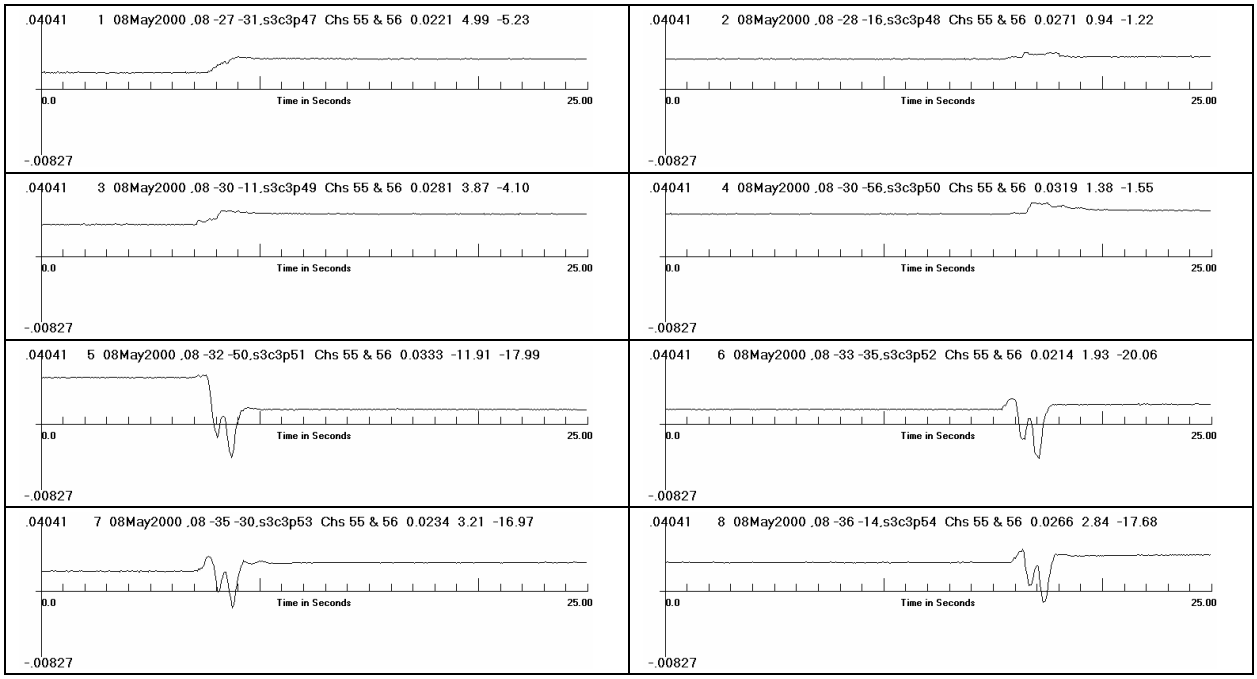

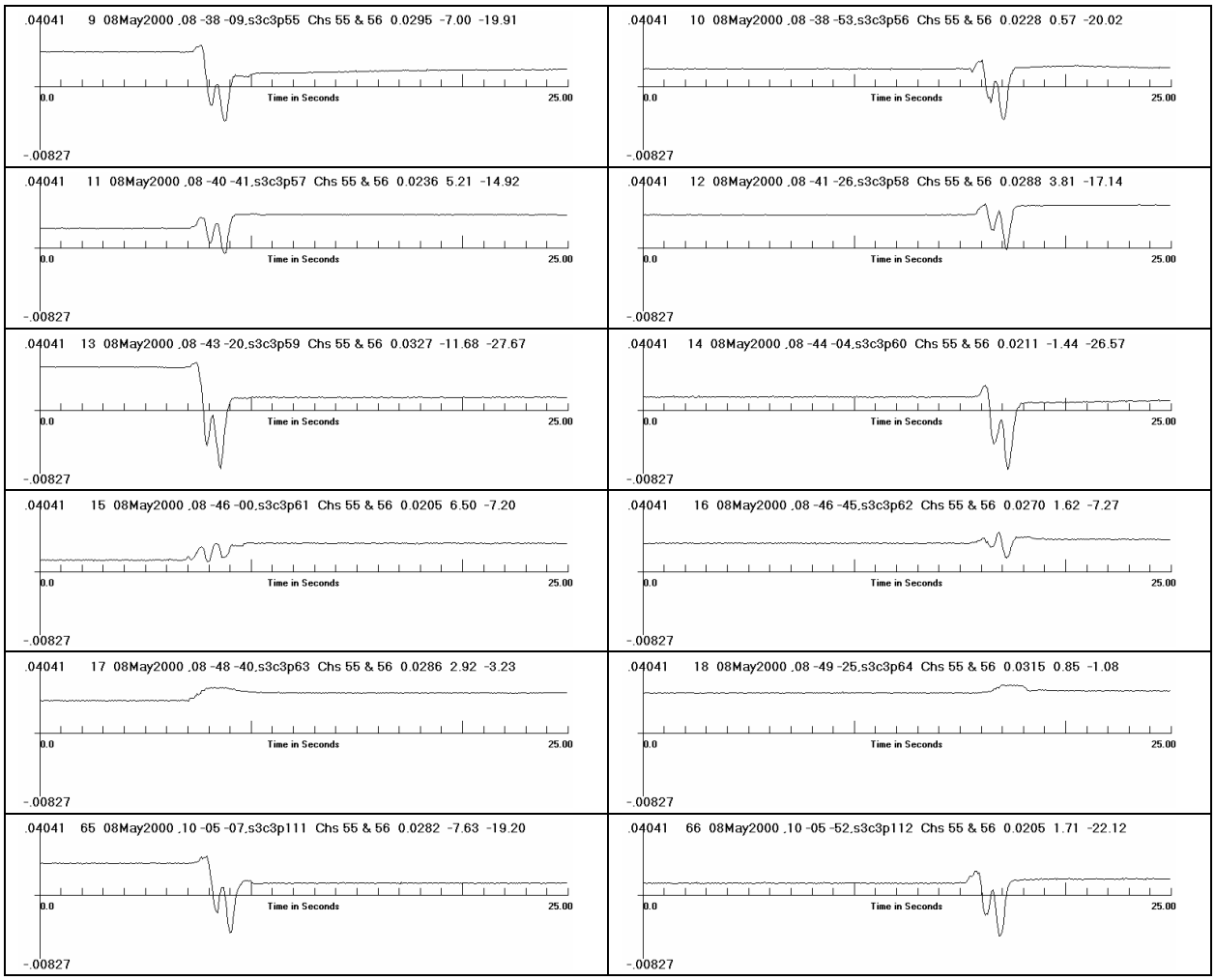

Figure 7. Time histories for relative displacement in the top 150 mm (6 in) of the subgrade under four-wheel loading. The left column is for the gear moving east and the right column is for the gear moving west. The last row gives the response at the last wander position (sequence numbers 65 and 66).

To check the repeatability of the strain measurements, the recovered and unrecovered strains were computed and plotted against wander position number for four consecutive wander cycles, starting on May 8, 2000, and finishing on May 10, 2000. The first wander cycle starts at pass number p47 (in the file name) and is the same wander cycle for May 8 as in figures 6 and 7. The last cycle, starting at p245, was interrupted at wander position 16 on May 8 and restarted at wander position 17 on May 10. Figures 8 through 11 are for six-wheel loading and figures 12 through 15 are for four-wheel loading.

The figures show that the measured recoverable strains were highly repeatable, both in absolute value and in the basic pattern from cycle to cycle. There appears to be a tendency for the largest recovered strain values to increase from the first to the last wander cycle, particularly for the four-wheel loading in figures 12, 13, and 14. This may be as much due to increase in temperature as the day progressed as to repeated loading. The standard deviation of the four data

points at each wander position was calculated for the strains in each of the figures. The standard deviations were then averaged over all wander positions in each figure. Table 2 shows the result.

The figures also demonstrate again that the recovered strains are essentially the same for travel in the east and west directions but that the unrecovered strains are different for travel in the two directions.

Table 2.
Variation in strain measurements averaged over all positions in four wander cycles. (SD = Standard Deviation.)

	Recovered Strain		Unrecovered Strain	
Loading Condition	Average SD, μStrain	SD as percent of maximum strain	Average SD, μStrain	SD as percent of maximum strain
6-Wheel East	142	3.6	142	14.2
6-Wheel West	109	2.7	110	36.7
4-Wheel East	151	3.0	147	4.9
4-Wheel West	176	3.5	111	11.1

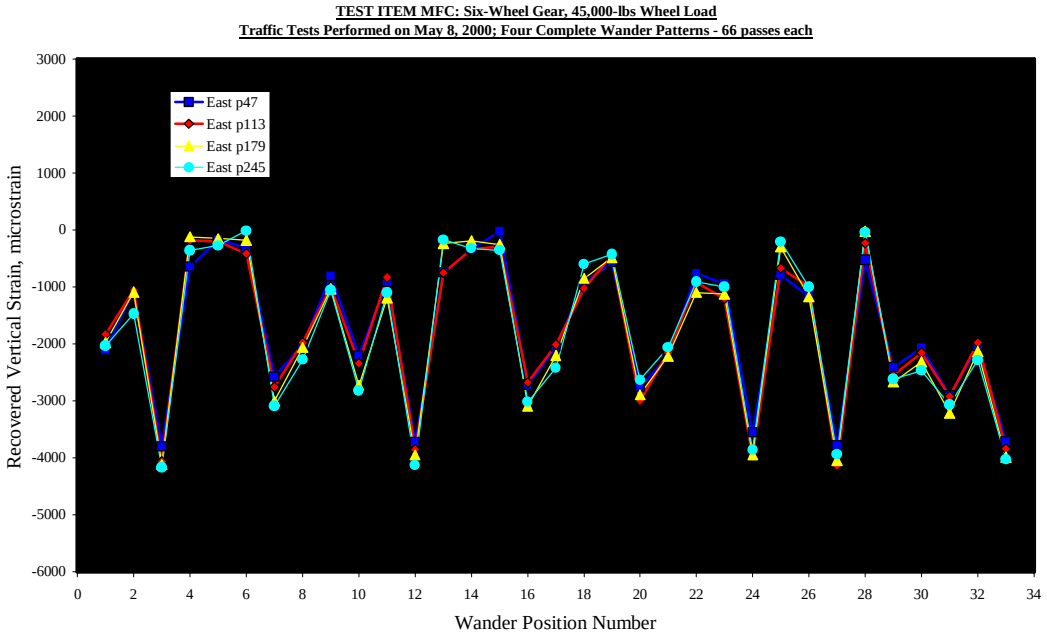

Figure 8. Recovered strains in the top 150 mm (6 in) of the subgrade over four consecutive wander cycles with travel in the east direction (new wander position each time). Six-wheel gear.

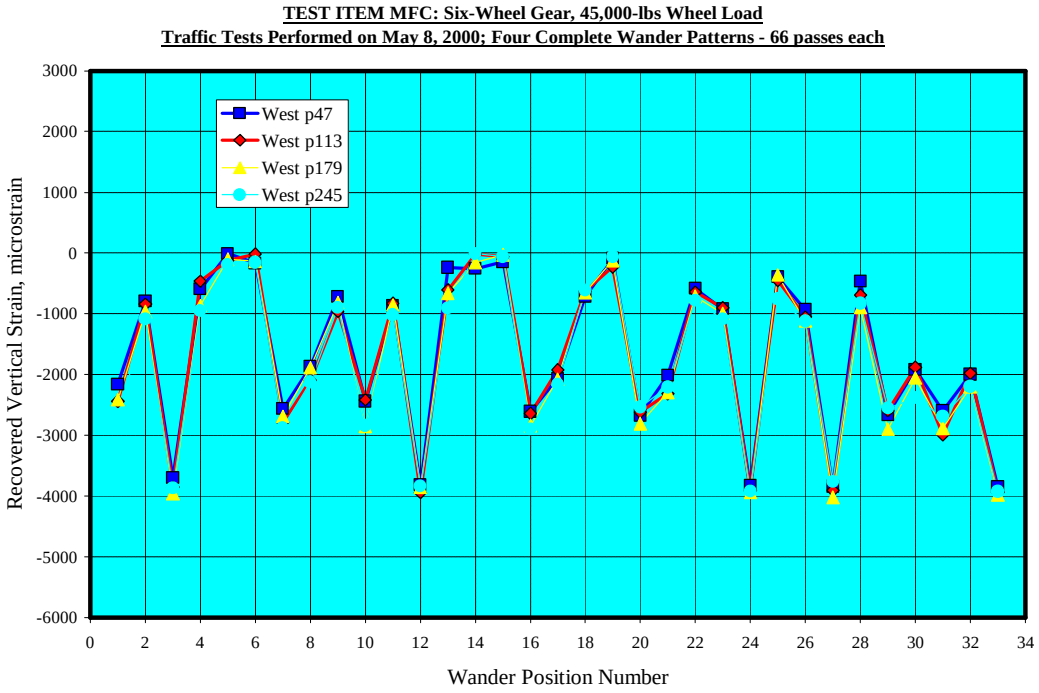

Figure 9. Recovered strains in the top 150 mm (6 in) of the subgrade over four consecutive wander cycles with travel in the west direction (same wander position as in the previous pass in the east direction). Six-wheel gear.

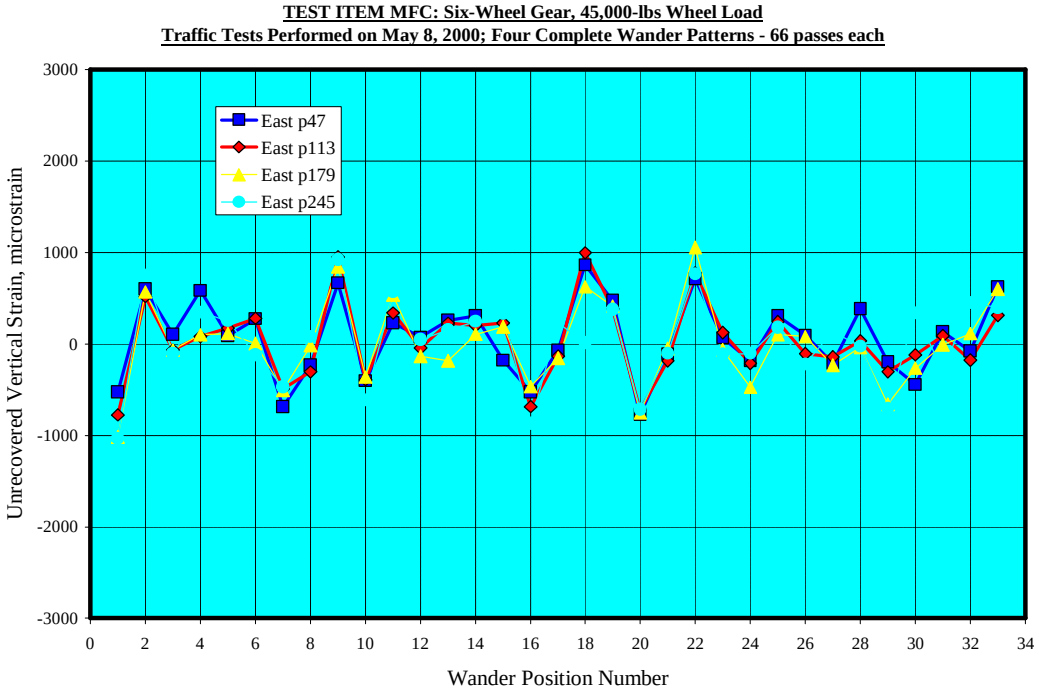

Figure 10. Unrecovered strains in the top 150 mm (6 in) of the subgrade over four consecutive wander cycles with travel in the east direction (new wander position each time). Six-wheel gear.

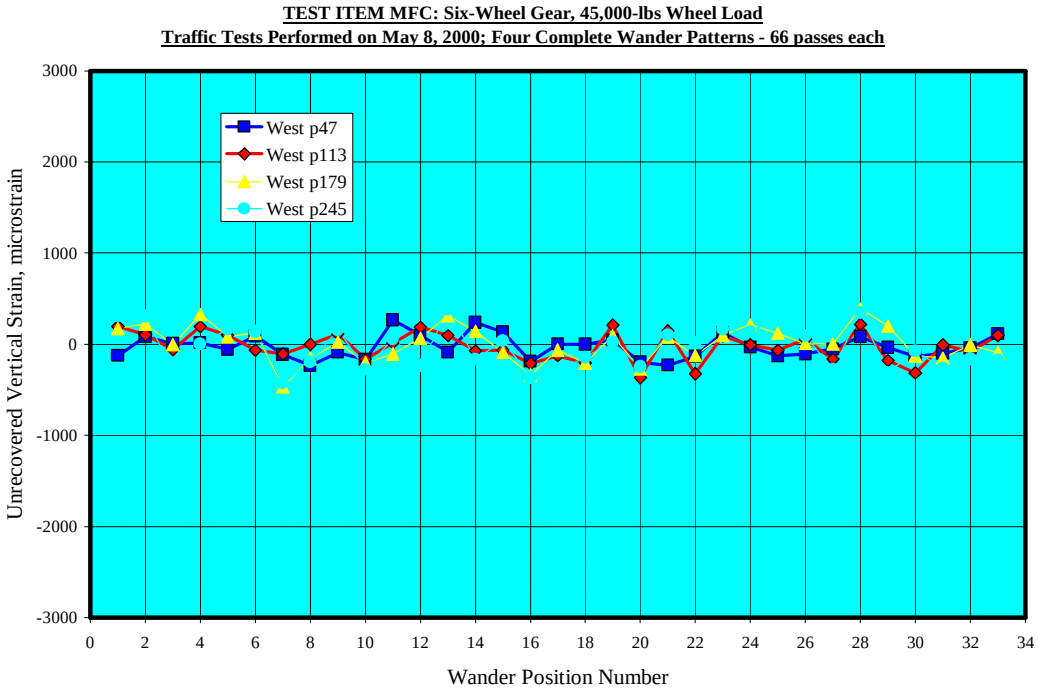

Figure 11. Unrecovered strains in the top 150 mm (6 in) of the subgrade over four consecutive wander cycles with travel in the west direction (same wander position as in the previous pass in the east direction). Six-wheel gear.

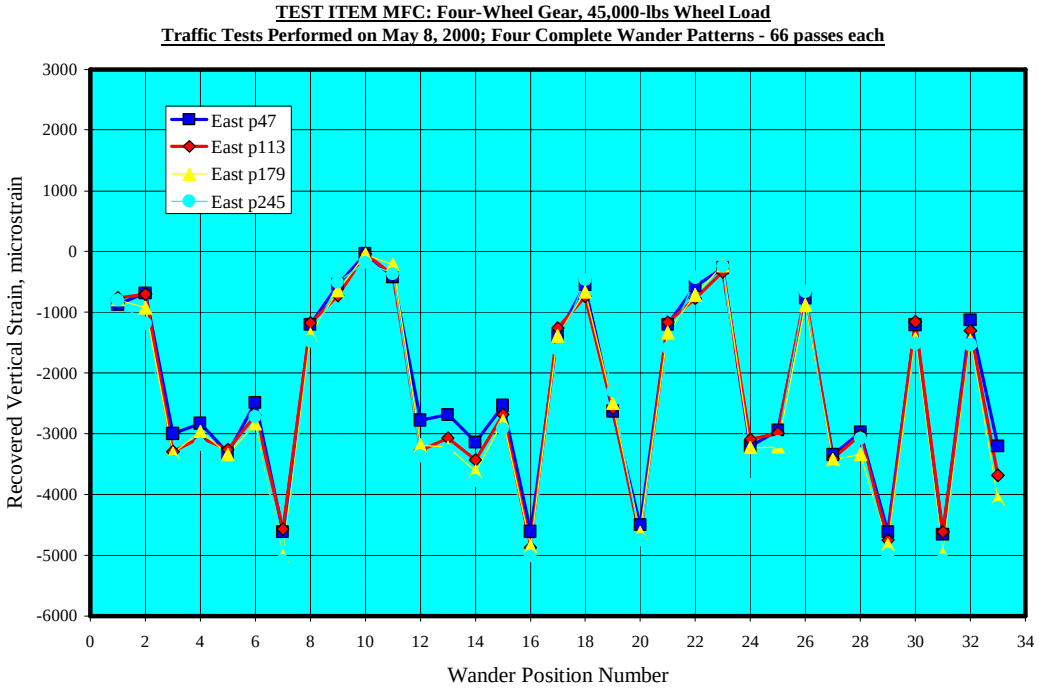

Figure 12. Recovered strains in the top 150 (6 in) mm of the subgrade over four consecutive wander cycles with travel in the east direction (new wander position each time). Four-wheel gear.

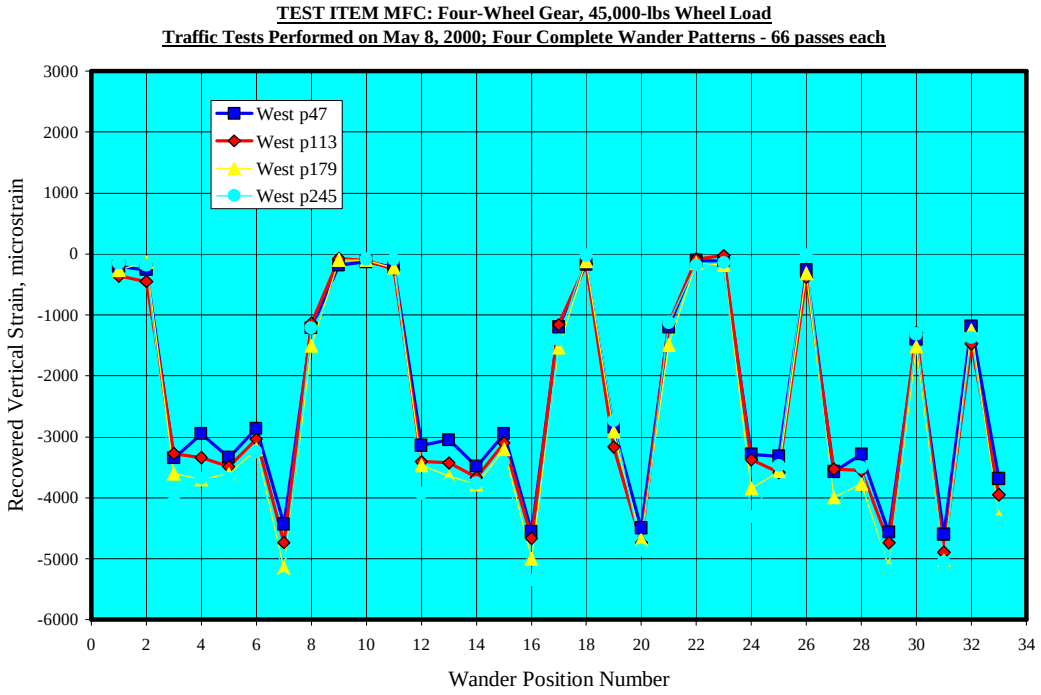

Figure 13. Recovered strains in the top 150 (6 in) mm of the subgrade over four consecutive wander cycles with travel in the west direction (same wander position as in the previous pass in the east direction). Four-wheel gear.

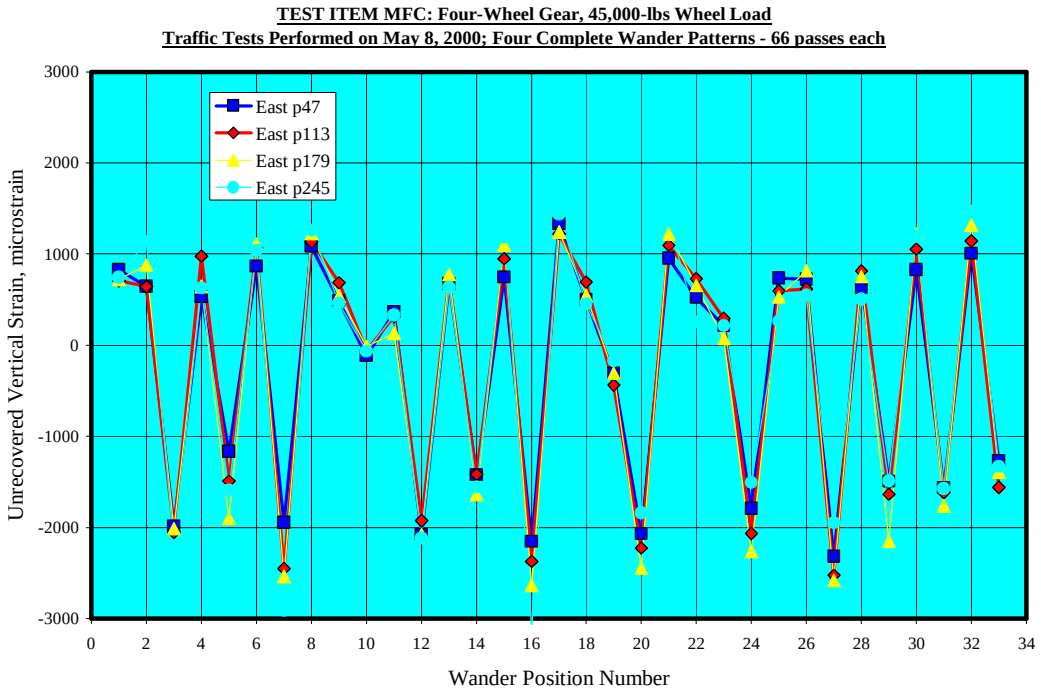

Figure 14. Unrecovered strains in the top 150 mm (6 in) of the subgrade over four consecutive wander cycles with travel in the east direction (new wander position each time). Four-wheel gear.

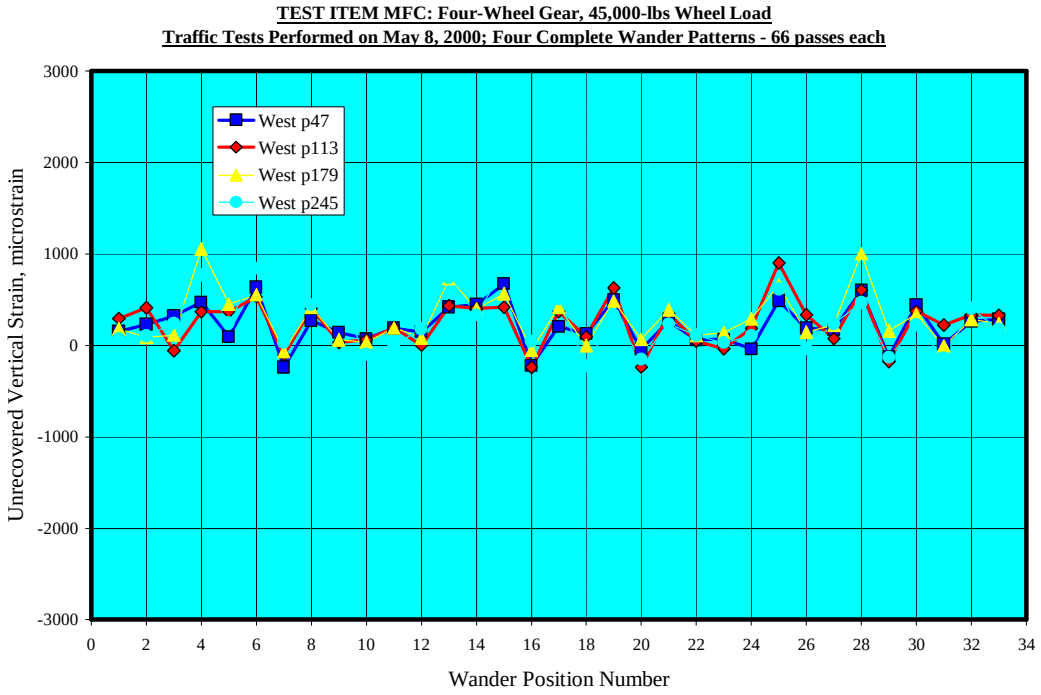

Figure 15. Unrecovered strains in the top 150 (6 in) mm of the subgrade over four consecutive wander cycles with travel in the west direction (same wander position as in the previous pass in the east direction). Four-wheel gear.

DATA QUALITY

The charts presented in the previous section show a high level of data quality over the four wander cycles selected for illustration. However, the hostile environment existing within the pavement and limited range of the sensors in the MDDs caused frequent degradations in the quality of the data collected from the MDDs.

Each of the seven sensors in one MDD had a separate cable with four conductors in a shielded case. The cables were collected into bundles laid just below the surface of the crushed aggregate material in the base layer. The cables were then lead across the transition section to the side of the test pavement and through a conduit into the data acquisition cabinet. Repeated loading of the test pavement, together with shear deformation within the base layer, tended to cause shorts within the cables. Some of the sensors therefore became inoperative as testing progressed. When an inoperative sensor was detected, the cable for that sensor was disconnected at the input to the data acquisition system. But before detection, the sensor typically provided a signal heavily contaminated by noise due to the shorting, causing the collection of invalid data records. In some cases, a sensor cable would short only when the load was applied in a few wander positions. In these cases the sensor might be left connected so that valid data could be collected at the other wander positions for as long as possible.

The sensors in the MDDs were potentiometers with a range of 25.4 mm (1 inch). As rut depth in the wheel tracks increased, the potentiometers exceeded their available range and many records were collected with the sensor output clipping when the wander position caused the largest response to the load. When clipping was detected, the potentiometers were adjusted to

bring them back into range. If there was no further adjustment remaining, the cable for that particular sensor was either disconnected completely or left connected so that data could be collected for those wander position not causing clipping.

It is important to be aware of these deficiencies in the data collected from the MDDs when analyzing the data. At present, the only way to detect whether the data is valid or not is by visual inspection of the individual data records, or by inspecting the reduced data for unreasonable changes in historical trends. Instances of invalid, or reduced quality, data are identified where applicable below.

STRAIN RESPONSE RECORDS OVER THE LIFE OF THE TEST ITEM

Figure 16 shows response time histories of the difference between the two sensors in the top 150 mm (6 in) of the subgrade in MDD2 for travel in the east direction. Six-wheel loading is on the left and four-wheel loading is on the right. The six-wheel time histories are for wander sequence number 5 (position number 3) and the four-wheel time histories are for wander sequence number 13 (position number 7). For these wander positions, one of the tandem sets of wheels on each gear passes directly over its respective MDD (see figure 5), typically giving the largest MDD displacements in the wander pattern. The time histories are for, top to bottom, repetition numbers 400, 3,700, 5,000, 8,300, 9,800, and 10,200. Rut depths at 10,200 repetitions, measured with a 3.7 m (12 ft) straightedge, were approximately 40 mm (1.6 in) and 66 mm (2.6 in) for the six-wheel and four-wheel traffic paths respectively. The vertical axes of the plots are scaled to show almost the full response in each plot. The scale of the vertical axis is therefore different in each plot.

The measured recovered deflection for both six- and four-wheel gears is five times larger at close to complete failure (10,200 repetitions) than at the start of testing (400 repetitions). Unrecovered deflections for the six-wheel gear start at relatively small levels compared to the recovered deflection, but jump to being 40 percent of the recovered deflection at 8,300 repetitions (June 2, 2000). Thereafter, the unrecovered deflection remains at a large fraction of the recovered deflection. On the four-wheel side, the unrecovered deflection is always a large fraction of the recovered deflection. (Variations in the responses as functions of the number of load repetitions are examined in more detail later.)

The six-wheel plot for June 14, 2000, has a reversal at the third peak which is not evident on plots for the other dates. This reversal is caused by channel 32 running out of available range and causing clipping of the electrical signal. Figure 17 shows plots of channels 32 and 34. Channel 34 is the deflection of a point 25 mm (1 inch) below the surface of the subgrade relative to the surface of the pavement and channel 32 is the deflection of a point 178 mm (7 in) below the surface of the subgrade relative to the surface of the pavement. Channel 34 subtracted from channel 32 gives the relative deflection in the (approximately) top 150 mm (6 in) of the subgrade as shown in figure 16. The value of the third peak of channel 32 is -1.0001 inch and the plot clearly shows clipping of the signal. The relatively small amount of clipping of channel 32 translates into a relatively large error in the last plot of figure 16 after subtracting channel 34. Figure 17 also shows the separate channels for the four-wheel side, channels 55 and 56. Although channel 55 peaks at a measured value greater than 1 inch (25.4 mm), the plot does not show clear evidence of clipping in the signal and the potentiometer reaches its maximum deflection for only a small period.

Figure 18 shows plots of the responses during the westward repetitions which followed the eastward repetitions of figure 16. Recovered deflections increase in magnitude with number of repetitions in the same manner as in figure 16, but the unrecovered deflections are uniformly small compared to the recovered deflections. Limiting is now clearly occurring in the signals for both of the gears at 10,200 repetitions. Channels 32, 34, 55, and 56 are isolated in figure 19 to show limiting of the individual sensor signals.

Isolation of the individual sensor signals in figures 17 and 19 is also of interest because the plots demonstrate that the aggregate base and subbase layers in the structure show the same response characteristics as the subgrade. That is, recovered deflections are of similar magnitude in both east and west travel directions, whereas unrecovered deflections are large compared to the recovered deflections in the east travel direction but are small in the west travel direction. Relative magnitudes, however, are different than for the subgrade, at least for the load applications shown.

A cause could not be found for the difference between the onset of large relative unrecovered deflections for the six- and four-wheel gear measurements. To check whether the difference may have been due to an anomaly in the structure or the MDD on the six-wheel side, responses from MDD1 in the north traffic lane were examined. Measurements from the sensor 25 mm (1 in) below the surface of the subgrade were not available for load repetitions up to 10,200, so the next lower pair (178 and 406 mm (7 and 16 in) below the top of the subgrade) were used to measure the average strain in the subgrade. Responses at the same load repetitions as in figures 16 and 18 are shown in figure 20. The response characteristics are the same as in figures 16 and 18 (for the six-wheel gear) except that the peaks are not as well defined. Unrecovered deflection increased from a small value at 5,000 repetitions (May 8) to 48 percent of the recovered deflection at 8,300 repetitions (June 2). Lower definition of the peaks is expected because the measurement is at a greater depth in the structure leading to more interaction between the responses from the individual wheel loads. A further difference is that MDD1 is at the west end of the test item. The MDD responses therefore start earlier in the response plots for eastward travel and later in the response plots for westward travel than is the case for responses from MDD2.

Figure 21 shows time histories of the relative deflection in the top 150 mm (6 in) of the subgrade for MDD1 on the four-wheel (south) side. Recovered deflections are somewhat less than those for the four-wheel gear in figures 16 and 18. Unrecovered deflection for eastward travel jumps in magnitude at a larger repetition number than for MDD2 on the four-wheel side, but at a smaller repetition number than for MDD2 on the six-wheel side. The differences in the onset of large unrecovered deflection in the subgrade therefore appear to be due to differences in the pavement structure at the different locations. Clipping in the responses for these channels was very severe after June 2, 2000, and the plots for responses after this date are not shown in figure 21.

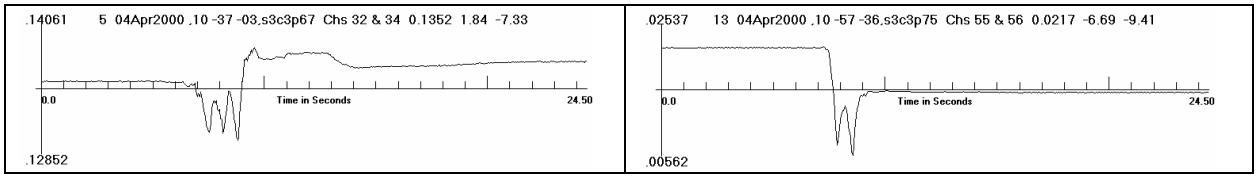

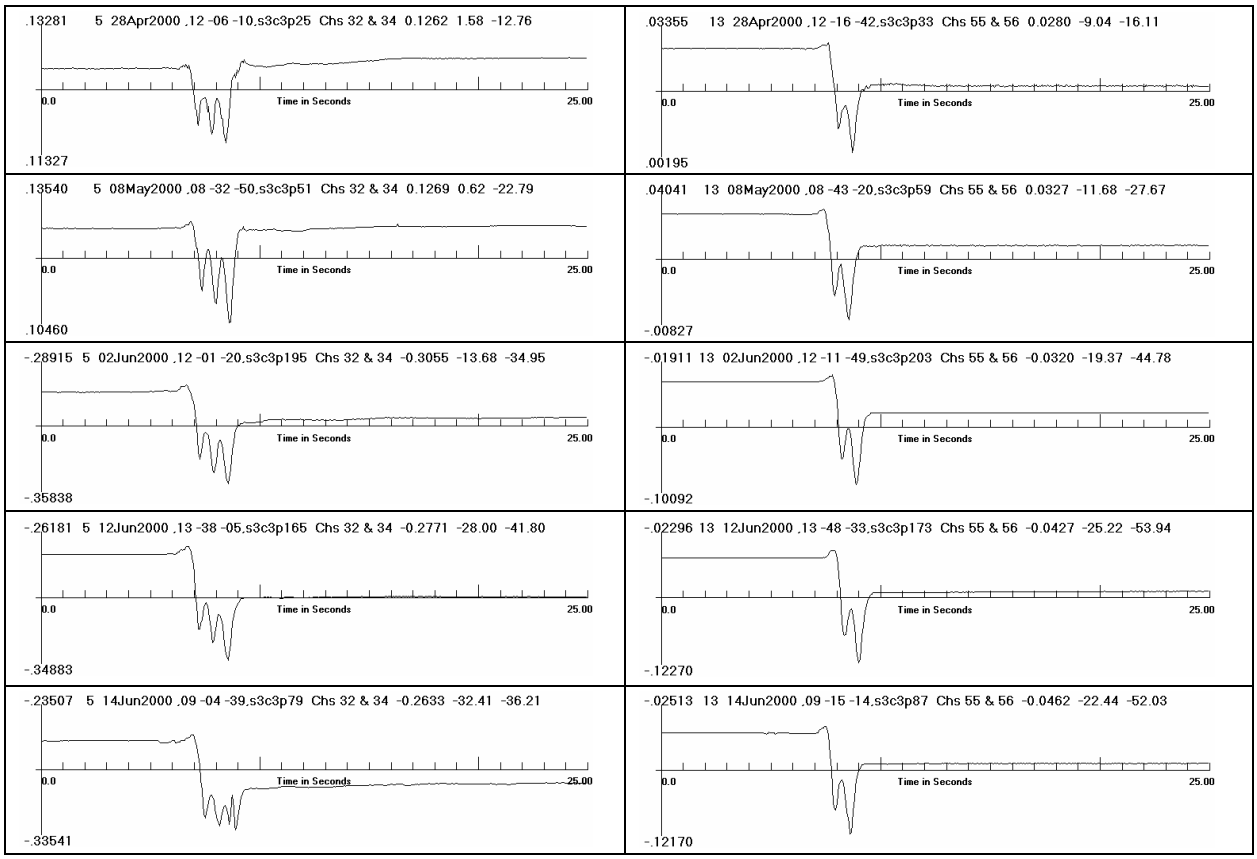

Figure 16. Relative displacements in the top 150 mm of the subgrade. Start of traffic to 10,200 repetitions shown top to bottom. Travel in the east direction (new wander position each time). Six-wheel is on the left and four-wheel is on the right.

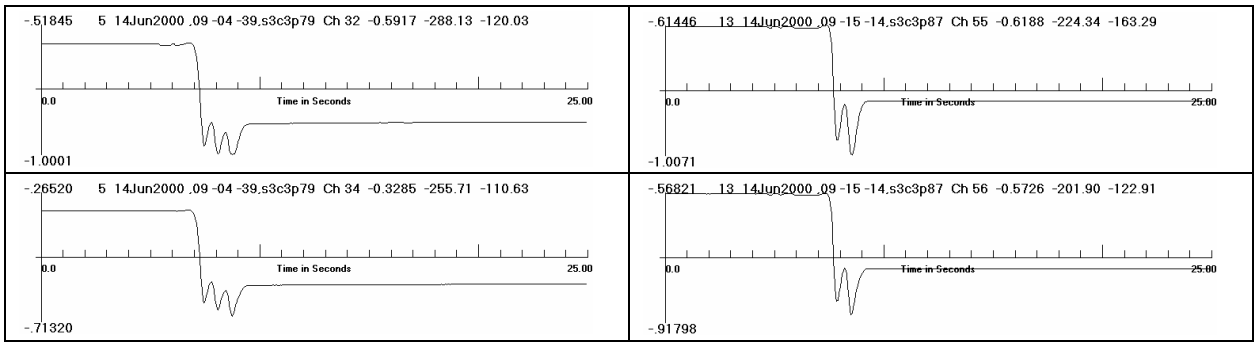

Figure 17. Subgrade displacements relative to the surface of the pavement at 10,200 repetitions showing clipping in channel 32 (same pass as in the last plot of figure 16). Travel in the east direction.

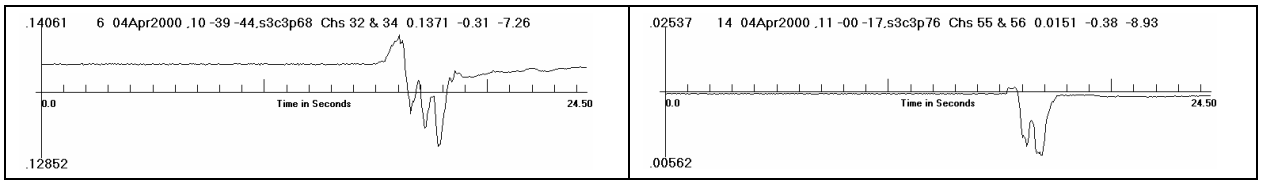

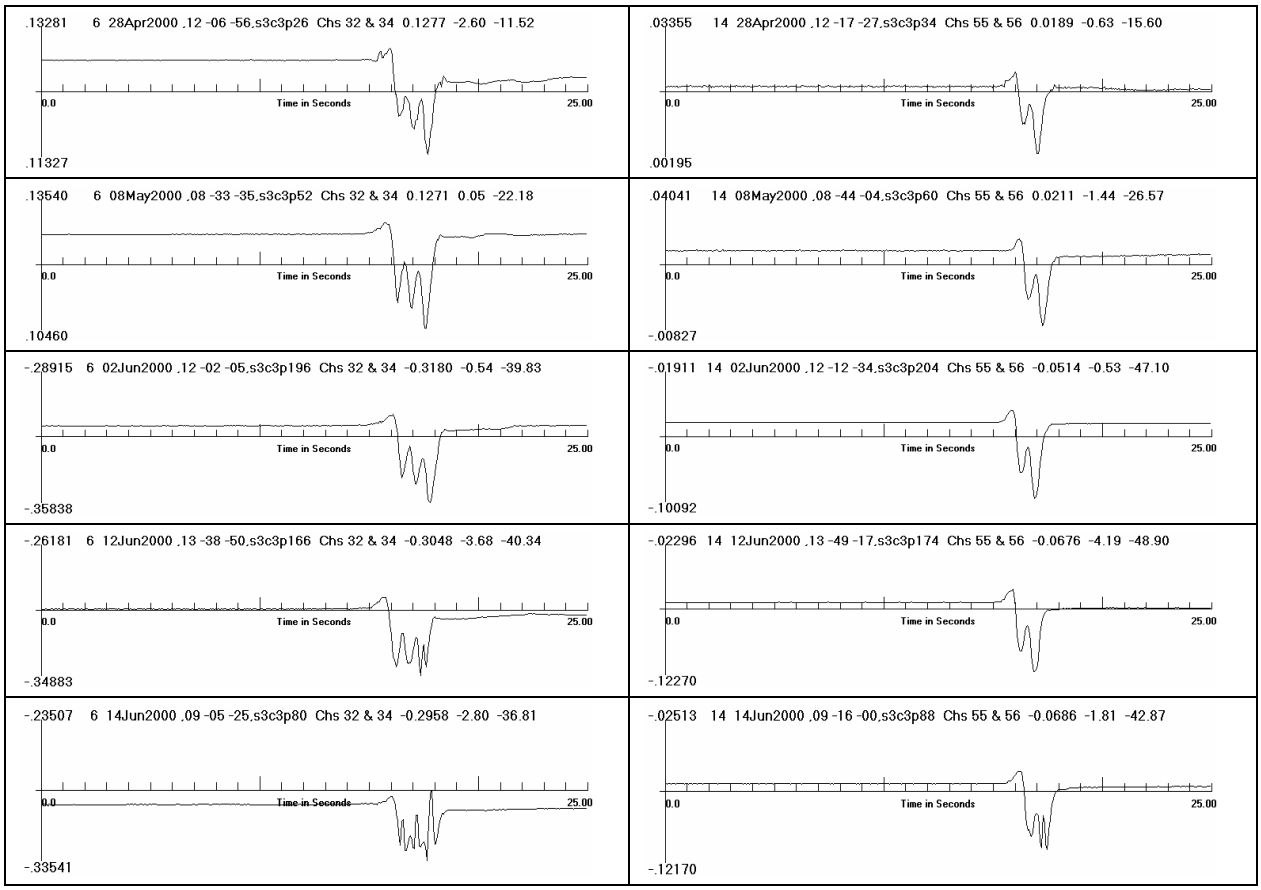

Figure 18. Relative displacements in the top 150 mm of the subgrade. Start of traffic to 10,200 repetitions shown top to bottom. Travel in the west direction (same wander position as in the previous pass in the east). Six-wheel is on the left and four-wheel is on the right.

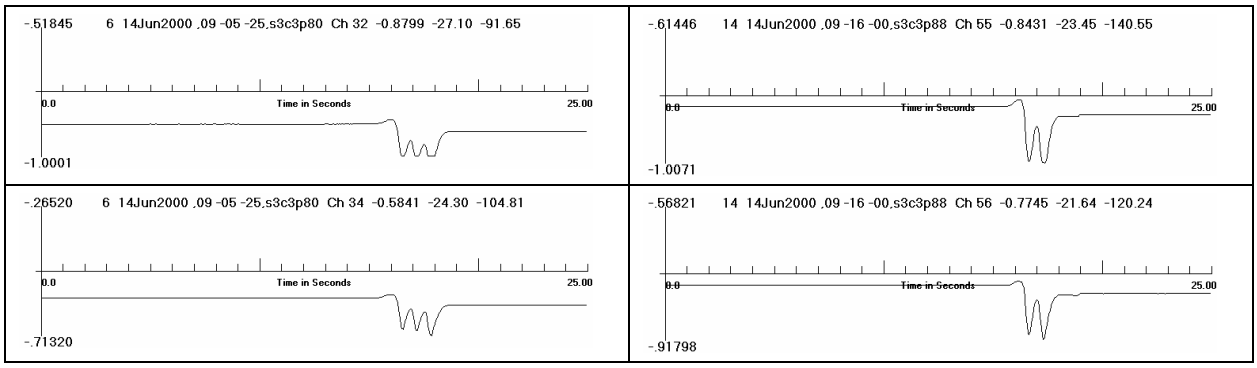

Figure 19. Subgrade displacements relative to the surface of the pavement at 10,200 repetitions showing clipping in channels 32 and 55 (same pass as in the last plot of figure 16). Travel in the west direction.

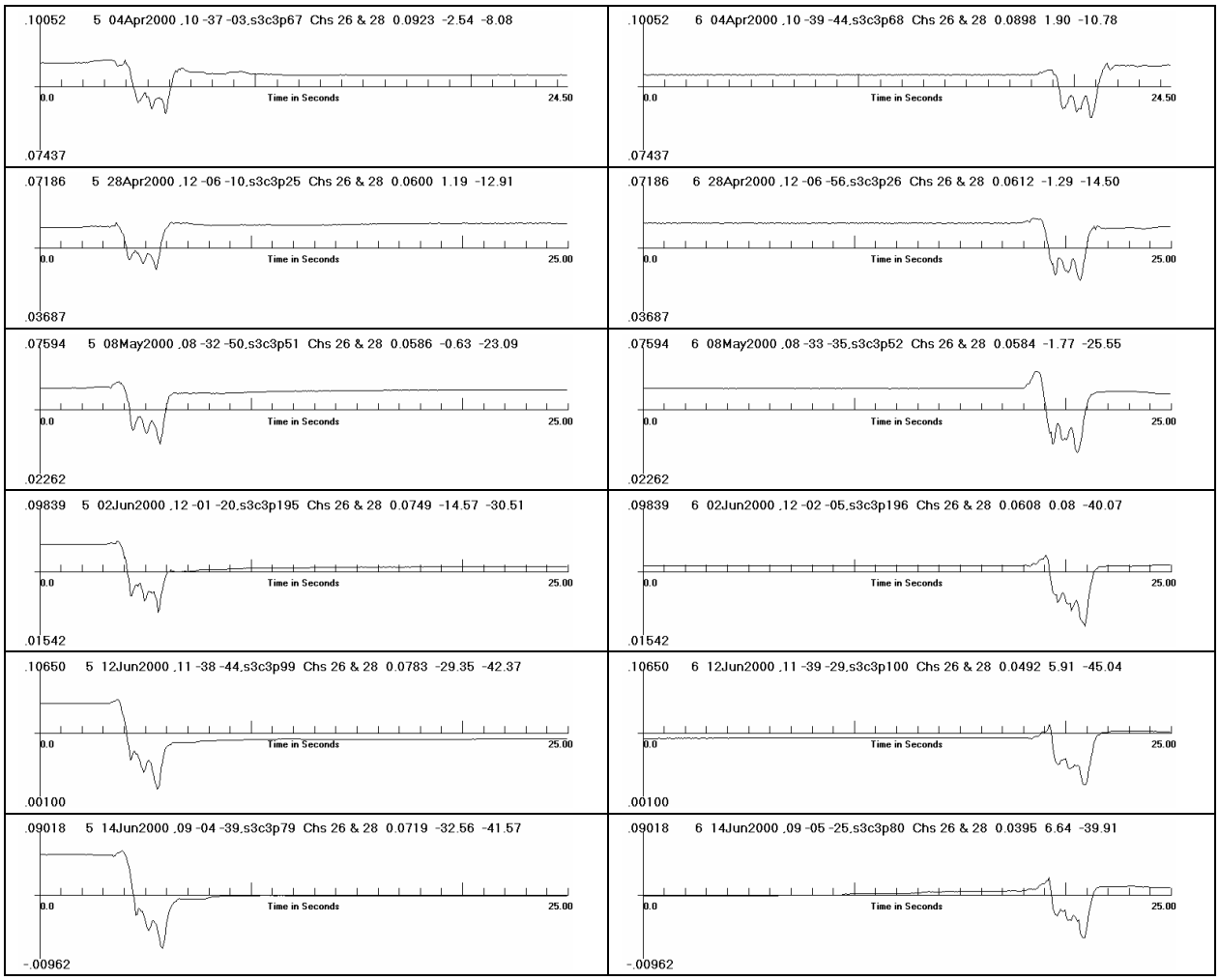

Figure 20. Relative displacement between points 178 and 406 mm (7 and 16 in) below the top of the subgrade for six-wheel traffic (MDD1). Start of traffic to 10,200 repetitions shown top to bottom. Travel in the east direction is on the left and west direction is on the right.

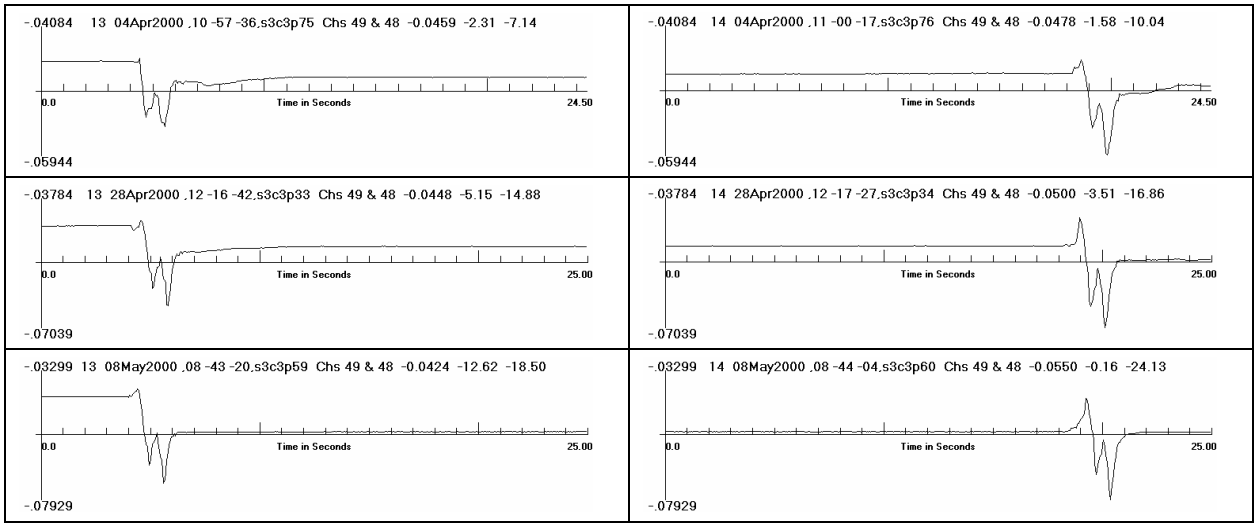

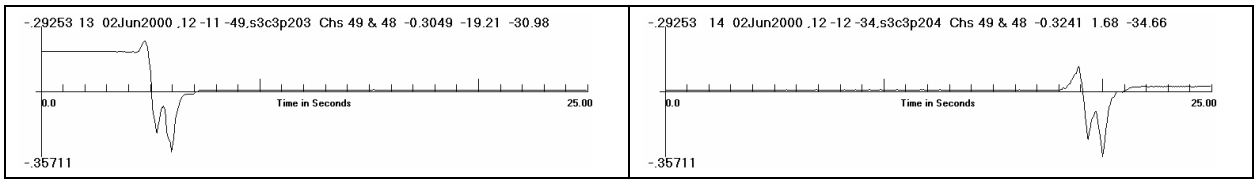

Figure 21. Relative displacement in the top 150 mm (6 in) of the subgrade for four-wheel traffic (MDD1). Start of traffic to 8,300 repetitions shown top to bottom. Travel in the east direction is on the left and travel in the west direction is on the right.

SUMMARY OF STRAIN MEASUREMENTS OVER THE LIFE OF THE TEST ITEM

The previous two sections presented detailed time histories of relative deflections (average strains) in the subgrade at a few wander positions and wander cycles. This section presents only the values of recovered and unrecovered strains. First, at all wander positions in six complete wander cycles over the life of the test item. Second, at one wander position in many wander cycles over the life of the test item.

Figures 22 through 27 show the recovered and unrecovered strains at each wander position in the same six wander cycles for which one time history per wander cycle is shown in figures 16 and 18. The strain measurements are also the same, being the average strain in the top 150 mm (6 in) of the subgrade at MDD2 north and south.

Figures 22 and 24 are for recovered strains with travel in the east direction for six- and four-wheel gears. Except for the wander cycle at 9,800 repetitions in figure 22, the patterns exhibited by the strains within each wander cycle are repeated very closely over all cycles from the first to the last. (Most of the measurements in the cycle at 9,800 repetitions were invalid because of what appeared to be random floating of one of the sensor outputs. The response at position number 3 shown in figure 16 just happened to give what appeared, visually, to be a reasonable result, with offsets matching before and after. The pattern in that region also matches that of the preceding cycles in figure 22.) Although the patterns are the same the magnitudes of the strains increase in the same manner as indicated previously. Some limiting was occurring in the cycle at 10,200 repetitions and this probably caused some clipping of the peak values in this wander cycle.

The patterns and magnitudes of the recovered strains for westward travel are very close to those in the east direction. Figure 25 is for the four-wheel case. Comparing figure 25 to figure 24, the last wander cycle has significantly smaller strain values for westward travel because of the clipping illustrated in figure 19.

Except for a couple of small expansive (positive) measurements in the first wander cycle, the recovered strains are always compressive (negative). The shapes of the patterns are different for the six- and four-wheel loading because of the different dual-wheel spacings and the different zero wander positions relative to the MDDs for the two load cases.

Figures 23 and 26 are for unrecovered strains with travel in the east direction for six- and four-wheel gears. Except for the wander cycle at 9,800 repetitions in figure 23, the patterns are repeated closely over all cycles from the first to the last, although not as closely as for the recovered strains. Repeatability becomes better as the strains increase in magnitude. The largest expansive strain measurements are of the same order of magnitude as the largest compressive strain measurements, as noted previously. The unrecovered strain response for travel in the west direction is completely different than for travel in the east direction. The four-wheel case is shown in figure 27. The magnitudes of the unrecovered strains are significantly lower than for

travel in the east direction and the patterns of the responses are not repeated as distinctly from cycle to cycle.

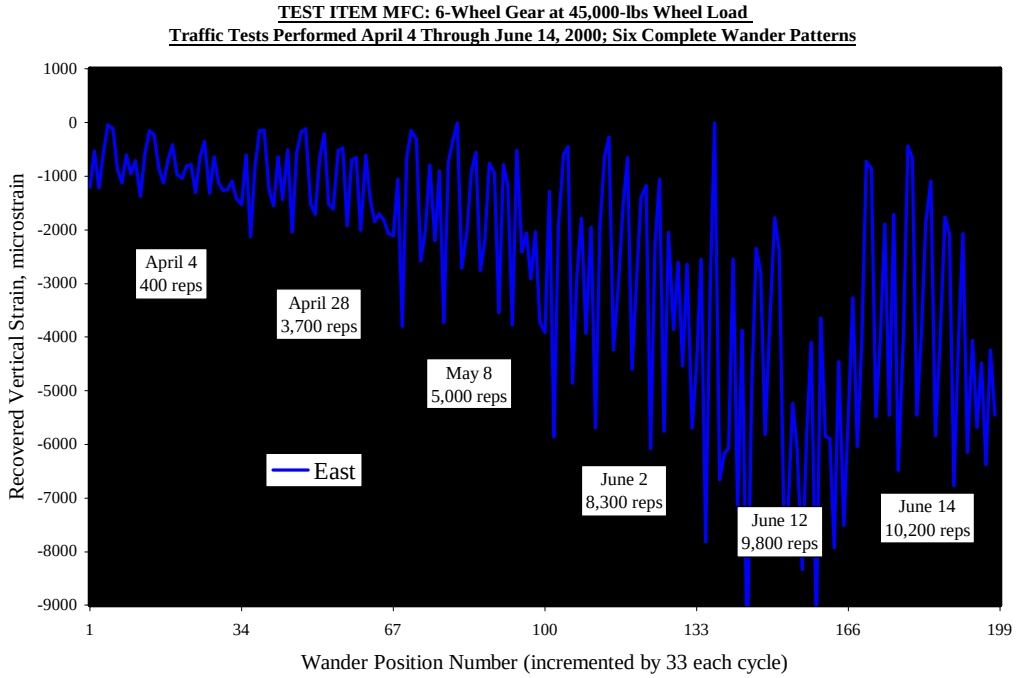

Figure 22. Recovered strains in the top 150 mm (6 in) of the subgrade for all wander positions in six complete wander cycles. East travel direction, six-wheel gear.

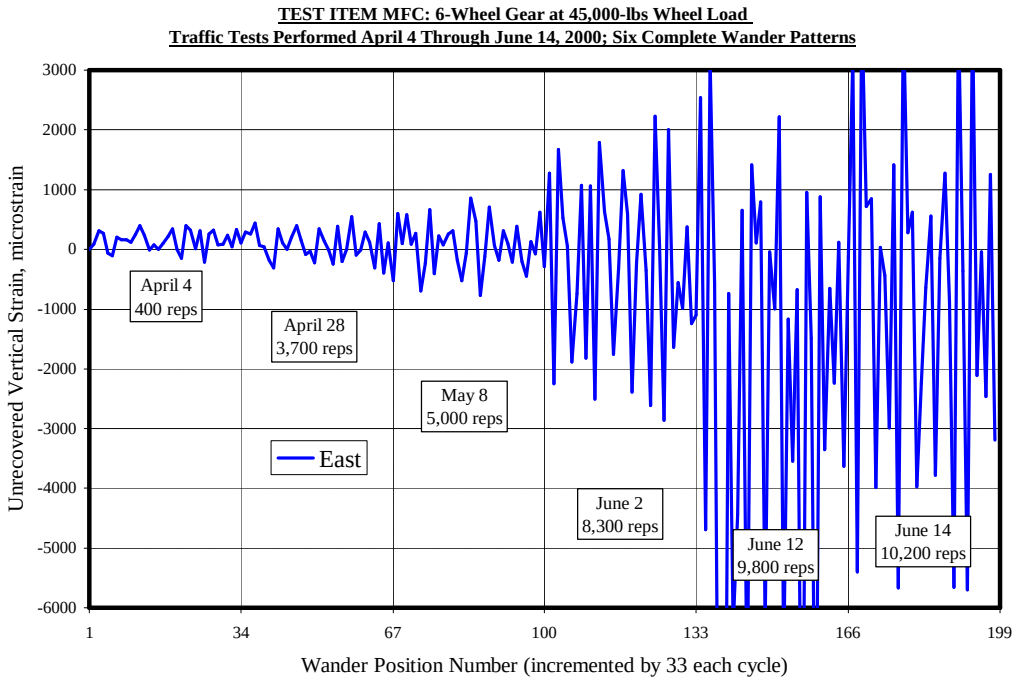

Figure 23. Unrecovered strains in the top 150 mm (6 in) of the subgrade for all wander positions in six complete wander cycles. East travel direction, six-wheel gear.

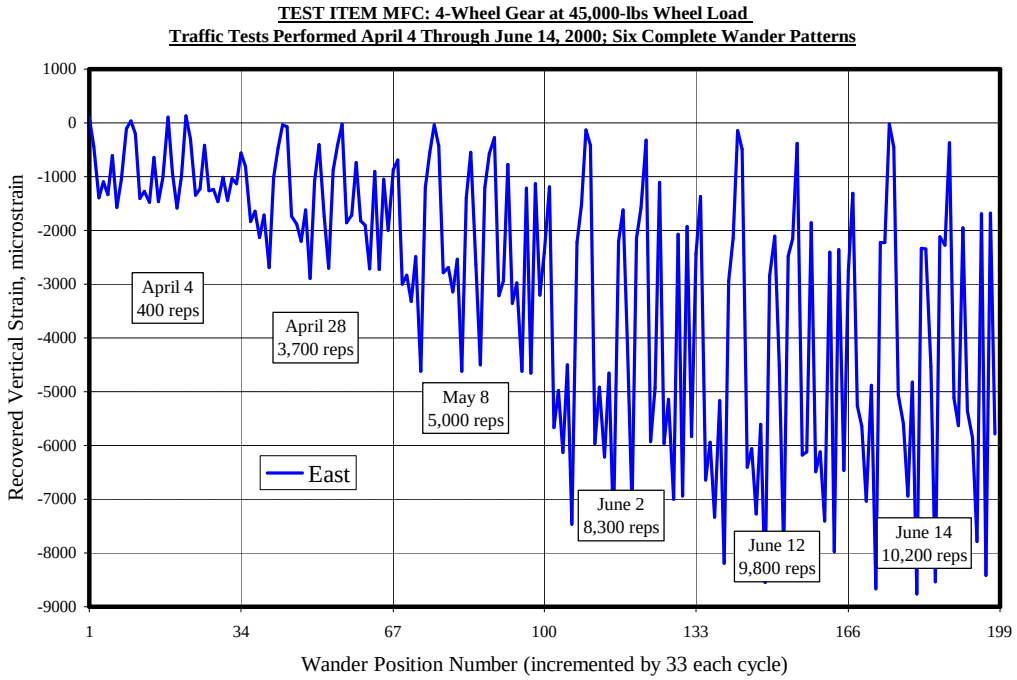

Figure 24. Recovered strains in the top 150 mm (6 in) of the subgrade for all wander positions in six complete wander cycles. East travel direction, four-wheel gear.

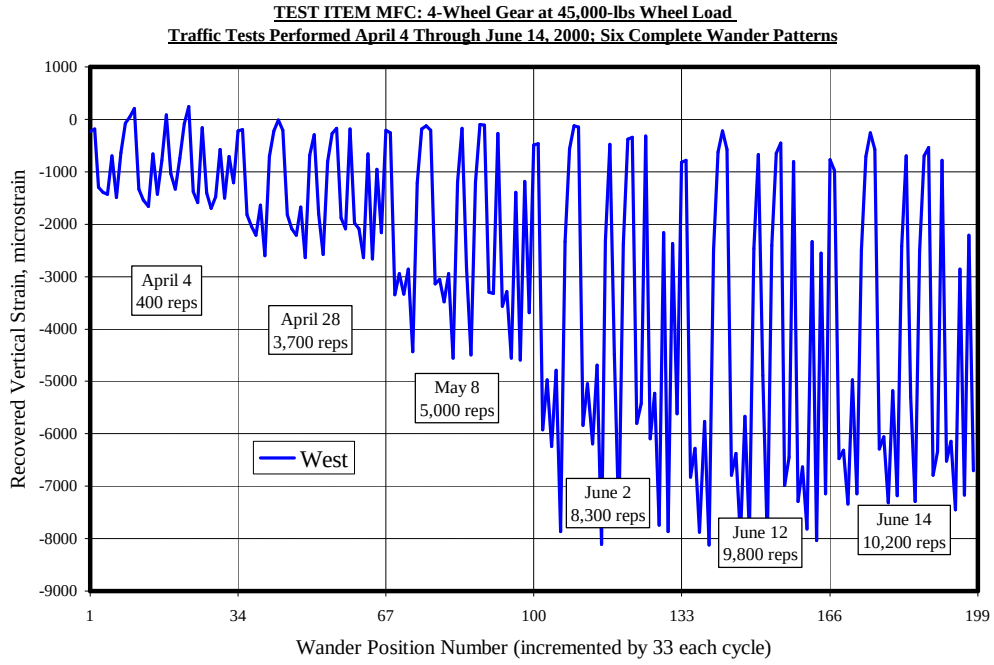

Figure 25. Recovered strains in the top 150 mm (6 in) of the subgrade for all wander positions in six complete wander cycles. West travel direction, four-wheel gear.

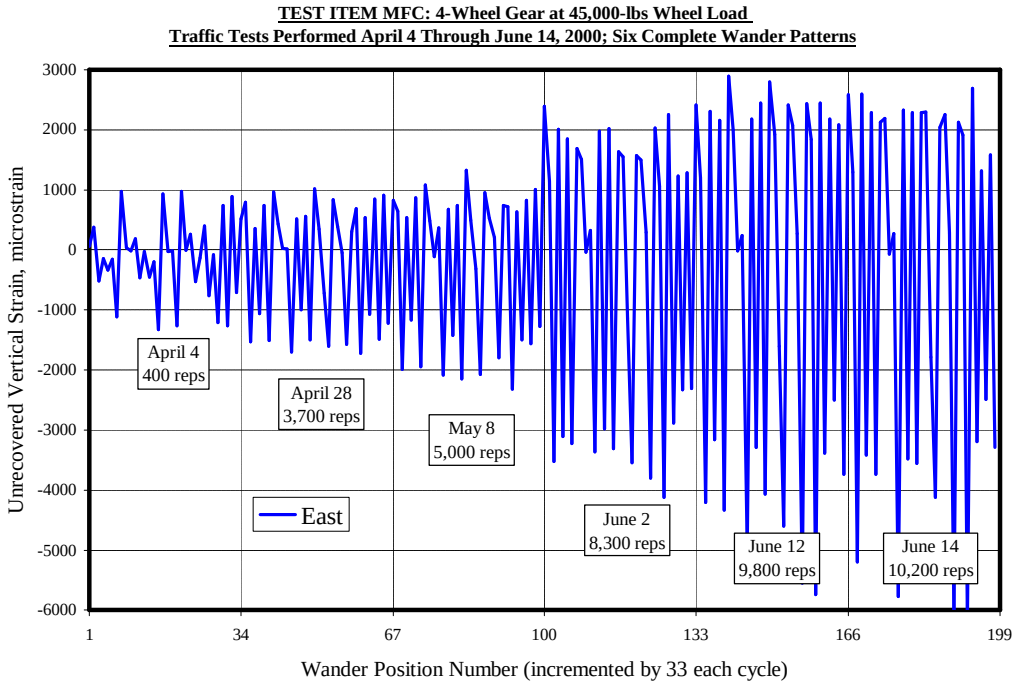

Figure 26. Unrecovered strains in the top 150 mm (6 in) of the subgrade for all wander positions in six complete wander cycles. East travel direction, four-wheel gear.

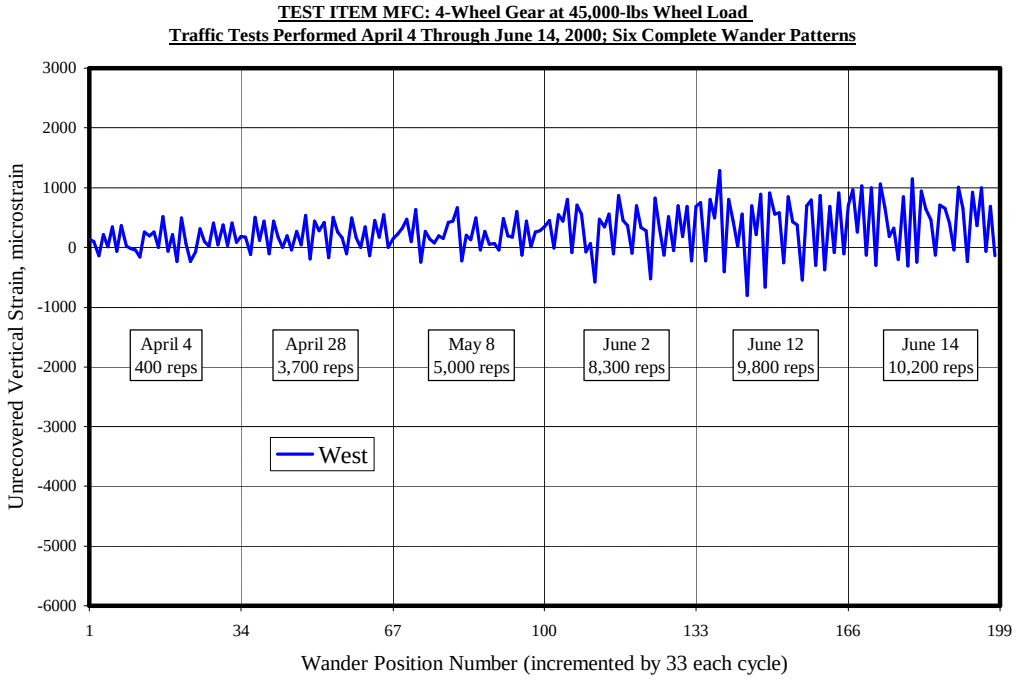

Figure 27. Unrecovered strains in the top 150 mm (6 in) of the subgrade for all wander positions in six complete wander cycles. West travel direction, four-wheel gear.

Figures 22 through 27 clearly indicate a trend of increasing subgrade strain response with deterioration in the condition of the pavement. To better examine the trend, figures 28 and 29 show the strain responses for six-wheel loading at wander position 3 in 37 wander cycles, and

figures 30 and 31 show the strain responses for four-wheel loading at wander position 7 in 42 wander cycles. These wander positions are for one set of tandem wheels passing directly over the MDDs and typically give close to the maximum strain response over a complete wander cycle. Figure 32 shows the average temperature in the asphalt surface layer of the test item (the individual temperatures at three different depths in the layer and in the two traffic paths can be found on website www.airporttech.tc.faa.gov).

Figure 28 is for six-wheel loading and travel in the east direction. The figure shows that the recovered strains increased approximately linearly as traffic increased from the start to about 2,000 repetitions. The recovered strains then remained essentially constant until about 4,000 repetitions. From 4,000 to about 6,500 repetitions the strains increased at a higher rate than in the first 2,000 repetitions. After 7,000 or 8,000 repetitions the measurements became unreliable due to offset drift and clipping as discussed previously. The individual records need to be visually inspected to determine the possible validity of the measurements in this region. For example, the measurements between 7,000 and 10,000 repetitions are probably valid, whereas the measurements after 10,000 were reading low because of clipping. The unrecovered strains were essentially constant, and close to zero, until just below 8,000 repetitions. After that the unrecovered strains increased, through to the last measurement, at about the same rate as for the recovered strains between 4,000 and 6,000 repetitions.

Figure 29 is for the same conditions but with travel in the west direction. The trends are almost exactly duplicated except that the unrecovered strains did not increase in magnitude after 8,000 repetitions.

The measured strains for the four-wheel case, shown in figures 30 and 31, also show the same basic trends except for the unrecovered strains in the east direction. These strains remained relatively constant until about 3,000 repetitions, after which the measurements increased in a somewhat erratic manner. Measurements in the region between 6,000 and 8,000 repetitions are somewhat unreliable though, due to clipping which started just before 6,000 repetitions and was fixed at 8,000 repetitions by adjusting the sensors. The clipping is reflected in the recovered strain measurements by an upward shift in the trend in the region between 6,000 and 8,000 repetitions.

The temperature of the asphalt, as shown in figure 32, was relatively constant at about 12 °C (53°F) until 4,000 repetitions. It then increased rapidly to about 18°C (65°F) at 5,000 repetitions, and remained fairly close to that value until it jumped to 21°C (70°F) at about 9,500 repetitions. The change in the rate of change of the recovered strains after 4,000 repetitions, as shown in figures 27 through 31, may be explained by the change in the temperature of the asphalt at 4,000 repetitions. The same kind of behavior has also been seen in the permanent deformation response of the surface of the flexible test items on the low-strength subgrade, only over a longer period of time. In these cases, the permanent deformation of the surface response showed an increase in the rate of change when the temperature increased and an arrestment of the permanent deformation when the temperature decreased. Detailed examination of the MDD responses for the low-strength subgrade test items is planned when time permits.

The results presented here should also be compared with the surface rutting measurements and the surface profile measurements made during trafficking of the MFC test item. Space does not, however, permit such a comparison in this paper.

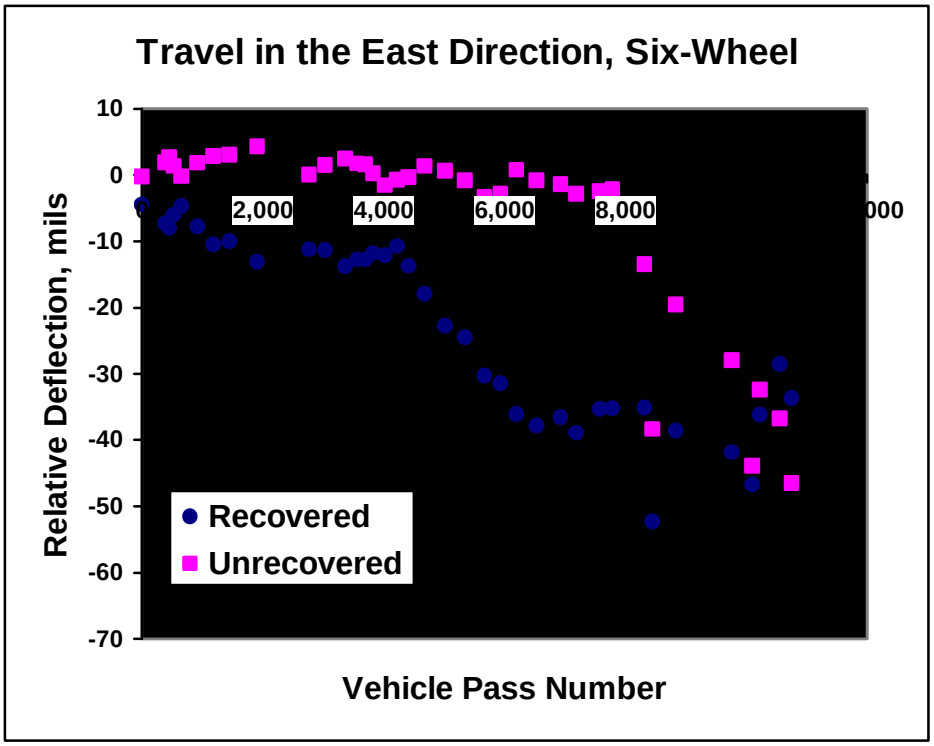

Figure 28. Strains in the top 150 mm (6 in) of the subgrade for wander position 3. Six-wheel gear traveling east. 1 mm = 39.4 mils.

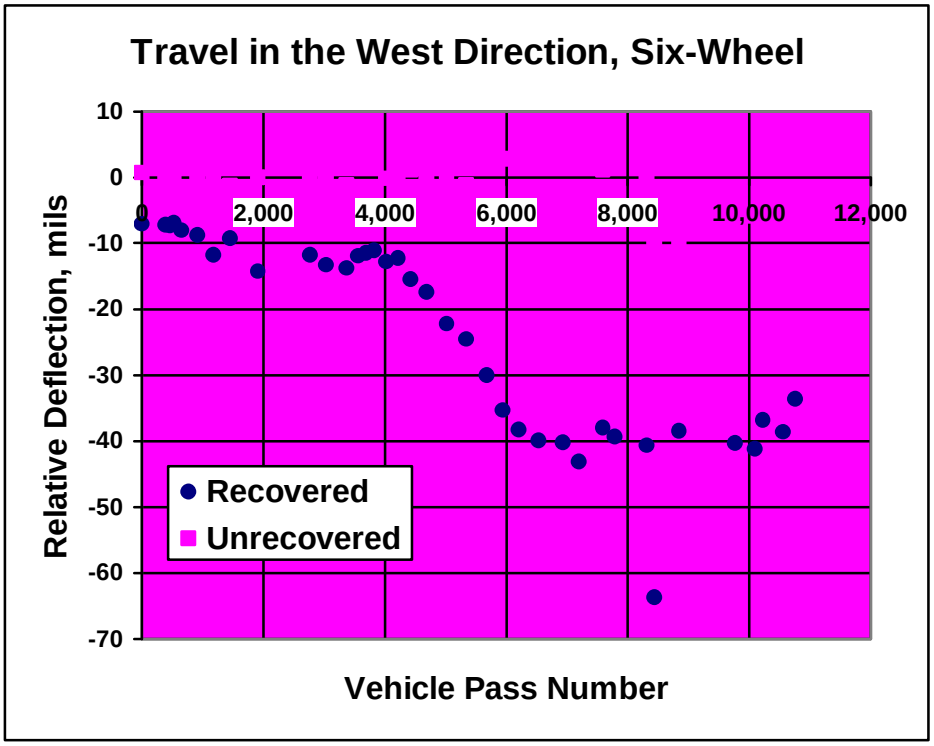

Figure 29. Strains in the top 150 mm (6 in) of the subgrade for wander position 3. Six-wheel gear traveling west. 1 mm = 39.4 mils.

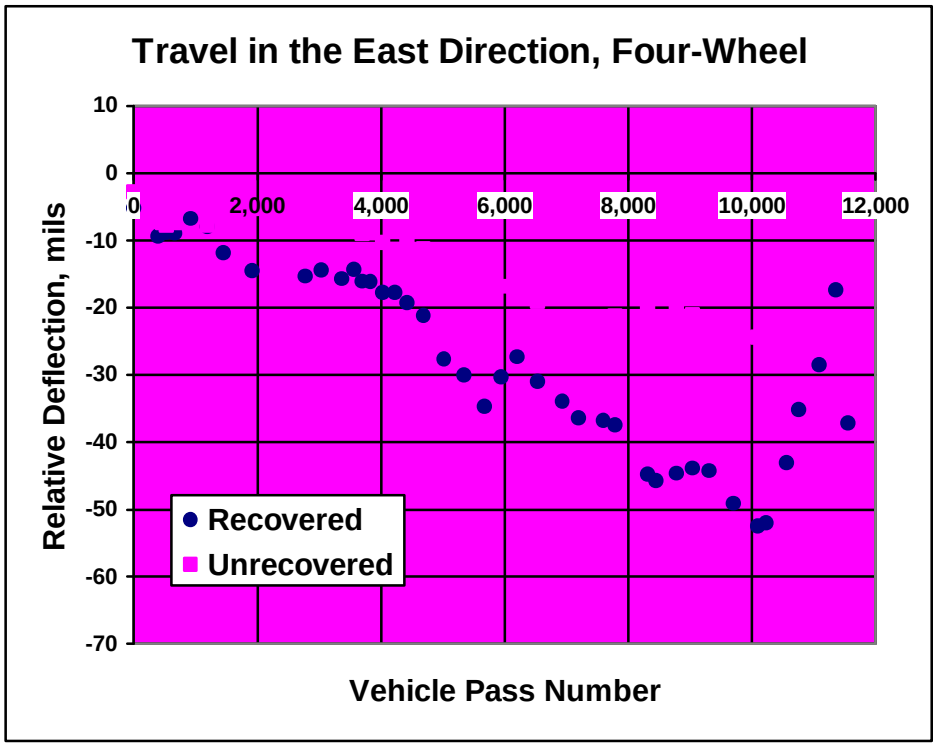

Figure 30. Strains in the top 150 mm (6 in) of the subgrade for wander position 7. Four-wheel gear traveling east. 1 mm = 39.4 mils.

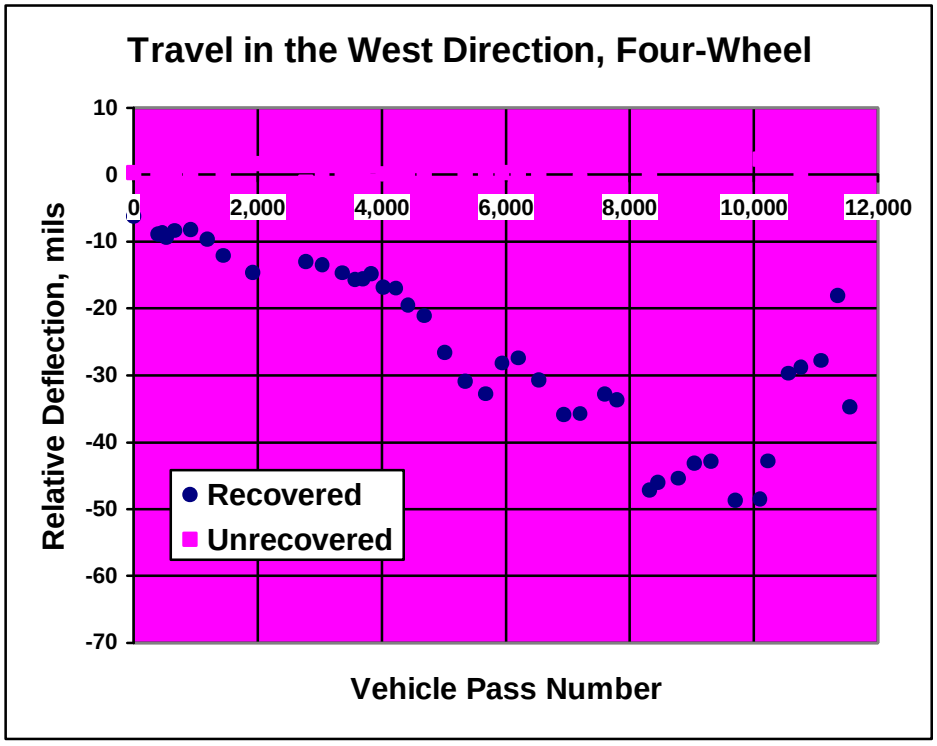

Figure 31. Strains in the top 150 mm (6 in) of the subgrade for wander position 7. Four-wheel gear traveling west. 1 mm = 39.4 mils.

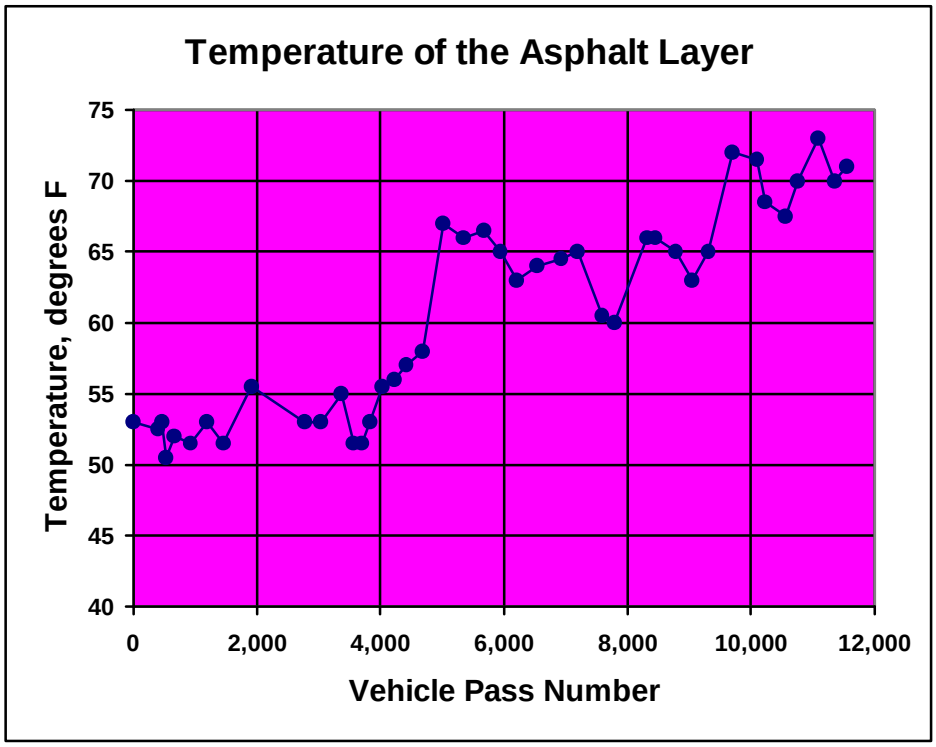

Figure 32. Average temperature in the asphalt layer of MFC versus repetition number.
1 °C = (1 °F - 32)/1.8

Results like those in figures 28 through 32 are more normally plotted with the horizontal axis on a logarithmic scale. Therefore, for the more normal view of the trends on semi-log plots, figures 28 through 32 are replotted in figures 33 through 37. The break in temperature at approximately 5,000 repetitions is also indicated on the additional plots by a vertical line.

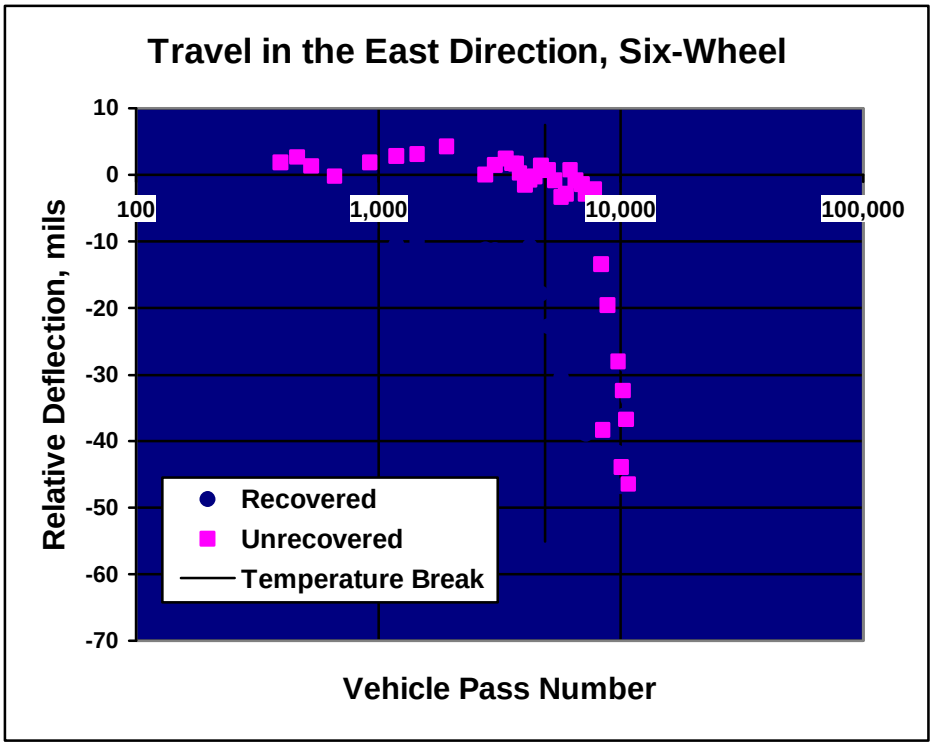

Figure 33. Strains in the top 150 mm (6 in) of the subgrade for wander position 3. Six-wheel gear traveling east. 1 mm = 39.4 mils.

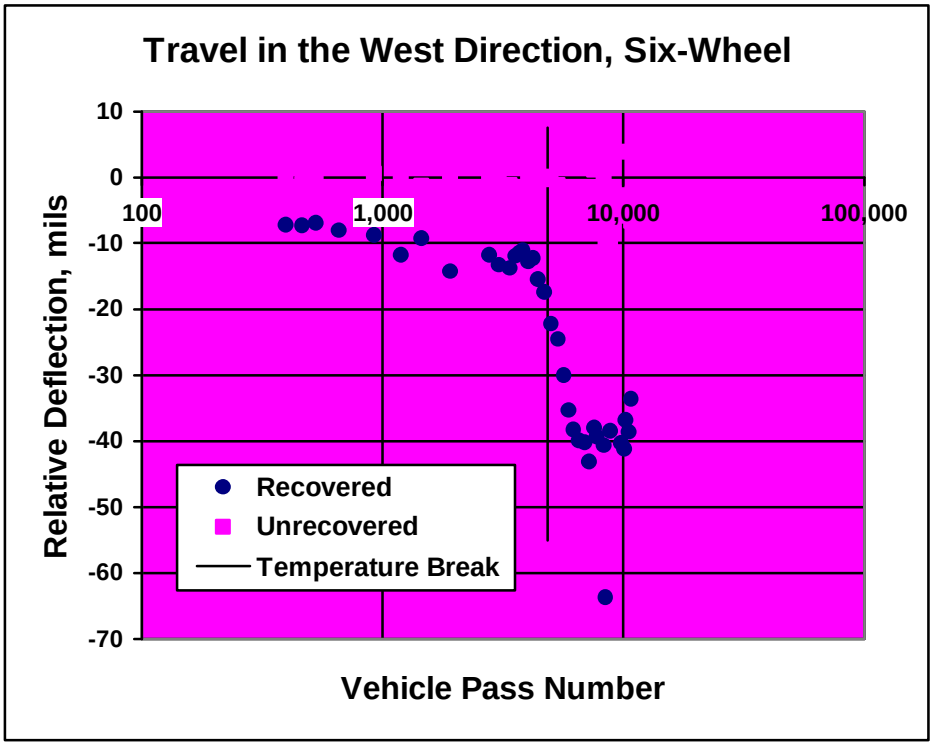

Figure 34. Strains in the top 150 mm (6 in) of the subgrade for wander position 3. Six-wheel gear traveling west. 1 mm = 39.4 mils.

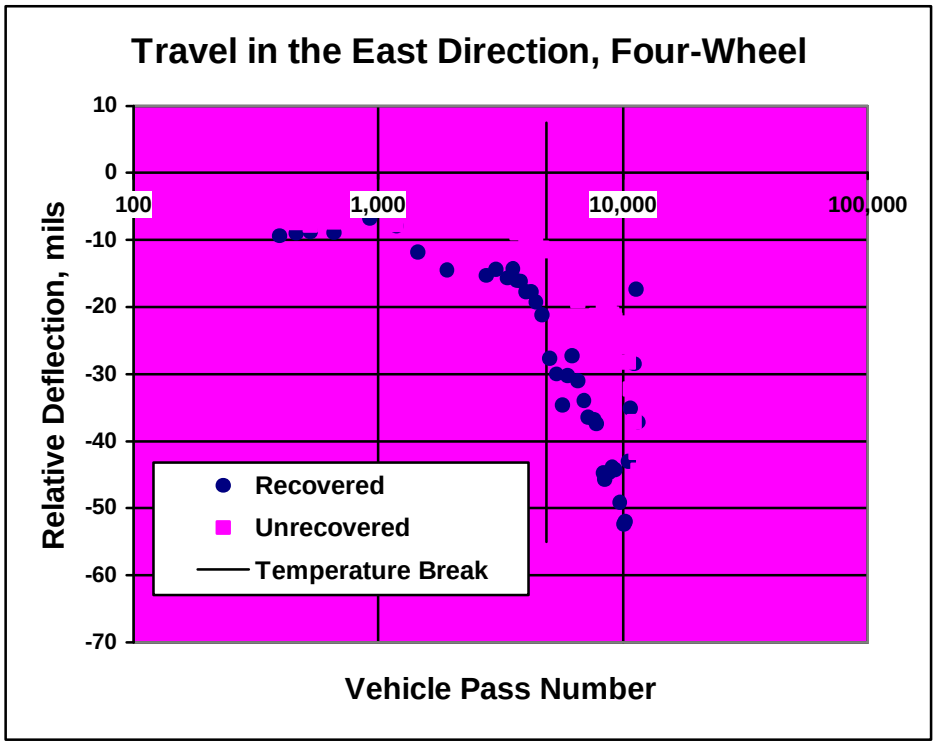

Figure 35. Strains in the top 150 mm (6 in) of the subgrade for wander position 7. Four-wheel gear traveling east. 1 mm = 39.4 mils.

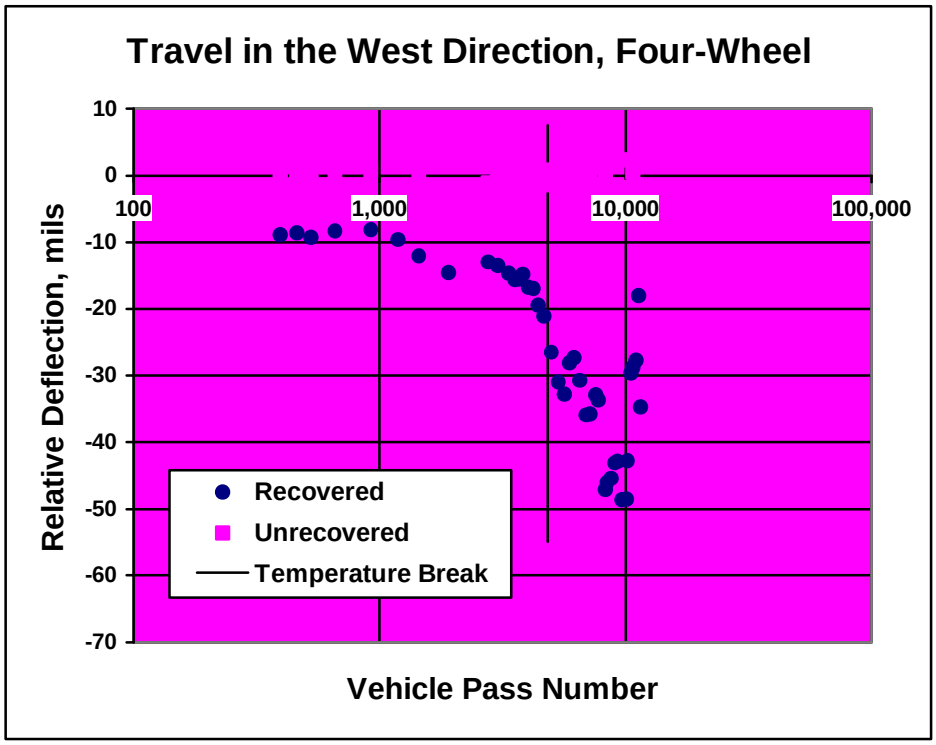

Figure 36. Strains in the top 150 mm (6 in) of the subgrade for wander position 7. Four-wheel gear traveling west. 1 mm = 39.4 mils.

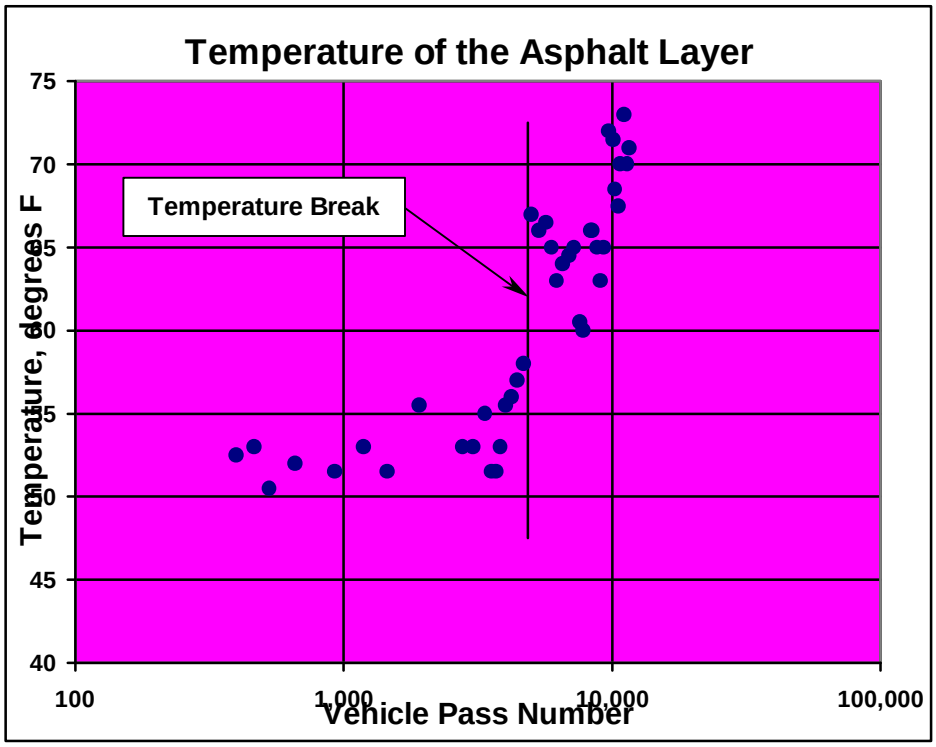

Figure 37. Average temperature in the asphalt layer of MFC versus repetition number.
1 °C = (1 °F - 32)/1.8

CONCLUSIONS

The average vertical strains in the top 150 mm (6 in) of the subgrade of a conventional flexible airport pavement structure were measured with multidepth deflectometers under traffic from full-scale six-wheel and four-wheel loads. The strain measurements demonstrated that the response of the pavement to simulated airplane loading is extremely complex. This conclusion is drawn from the following observations.

- Successive peak strain values from the passage of wheels in tandem shows increasing peak values from the first to the last of the wheel passes. The difference between the first and the last of the peaks is very significant and can be as large as the magnitude of the first peak. This behavior does not well represent the response of an assumed elastic structure or the response of a structure to a statically applied (nonmoving) load. In both cases the first and last peaks would be of the same magnitude. The effect is also most likely a function of speed. More analysis of the available data is required to investigate the effect of speed.
- Permanent deformation as evidenced by unrecovered vertical strains in the subgrade (and in aggregate layers) was a significant component in the total response of the pavement structure during the traffic tests.
- Recovered and unrecovered strains both increased significantly in magnitude as the condition of the pavement structure deteriorated.
- Recovered strains are very weakly dependent on the path of previously applied loads, whereas unrecovered strains are very strongly dependent on the path of previously applied loads. This demonstrates that the response of the pavement is strongly path dependent and

that wander is an important component in the loading applied to the pavement, at least for the wander pattern and range of transverse wheel paths used in the traffic tests. (The wander pattern used is representative of single aircraft operation on a taxiway except that nine fixed and equally spaced wheel paths were used instead of the randomly distributed pattern usually assumed for use in theoretical models.) Trafficking with wander is intrinsically different than trafficking with the load applied repeatedly along the same wheel path.

- The rate of change of the magnitude of the recovered strains with applied traffic was indicated to be strongly dependent on the temperature of the asphalt surface layer. This is to be expected considering that the stiffness of asphalt is strongly dependent on temperature. However, the effect appears to be stronger than expected and more investigation is required to further quantify the effect, for test design and planning as well as to understand the mechanisms involved. Note that there are no theoretical models existing that relate pavement structural deterioration of this kind to asphalt properties for multiwheel traffic loading with wander. Also, significant distress of the asphalt surface layer was not evident until close to complete structural failure.
- The onset of increase in the rate of change of unrecovered strains was different at different sections of the test item. The effect appeared to be dependent on differences in the pavement structure at the different sections rather than unreliability in the strain measurements or differences caused by the different gear geometries. A difference in the onset of increase in unrecovered strains was the main difference that was identified between pavement response to six- and four-wheel loading, except for three peaks in the recovered strain histories for six-wheel loading as opposed to two peaks for four-wheel loading. Differences in the magnitude of recovered strains in the subgrade of the MFC structure should not necessarily be expected because maximum vertical strain at the top of the subgrade is predicted by layered elastic models to be about the same for both wheel configurations. In fact, vertical strain at the top of the subgrade due to the four-wheel loading is predicted to be slightly higher than that due to the six-wheel loading. The close correspondence between strains from the two gears is due to the relative shallowness of the pavement structure and the closer dual spacing of the four-wheel gear.
- Net unrecovered strain over a complete wander cycle is very small both in absolute terms and relative to the unrecovered strains at individual wander positions. The net unrecovered strain over a single wander cycle represents the permanent deformation in the subgrade accumulated over that wander cycle. When accumulated over the complete test to failure, these small increments of permanent deformation represent the contribution of the subgrade to total rut accumulation.

Taken together, these observations indicate that a realistic theoretical model of flexible pavement response to airplane loading should include permanent deformation, moving loads with wander, repeated loading, and representation of structural parameters as functions of temperature and accumulation of damage.

ACKNOWLEDGEMENTS/DISCLAIMER

The work described in this paper was supported by the FAA Airport Technology Research and Development Branch, Dr. Satish K. Agrawal, Manager. The contents of the paper reflect the views of the authors, who are responsible for the facts and accuracy of the data presented within.

The contents do not necessarily reflect the official views and policies of the FAA. The paper does not constitute a standard, specification, or regulation. Thanks are also due to Richard G. Ahlvin for his continued help and advice.

KEYWORDS

Airport Pavement, Flexible pavement, Full-scale tests, Multidepth-deflectometer, Subgrade strain.

REFERENCES

1. Federal Aviation Administration, Office of Airport Safety and Standards, "Standards for Specifying Construction of Airports," Advisory Circular AC 150/5370-10A, U.S. Department of Transportation, 1989 (also see http://www.faa.gov/arp/150acs.htm for updates).
2. R.G. Ahlvin, H.H. Ulery, R.L. Hutchinson, and J.L. Rice, "Multiple-Wheel Heavy Gear Load Pavement Tests Volume 1 Basic Report," Technical Report S-71-17, U.S. Army Engineer Waterways Experiment Station, November, 1971.
3. Navneet Garg, "Posttraffic Testing at the National Airport Pavement Test Facility: Test Item MFC," Report DOT/FAA/AR-TN01/49, U.S. Department of Transportation, Federal Aviation Administration, September, 2001.
4. Richard H. Ledbetter, "Pavement Response to Aircraft Dynamic Loads Volume II Presentation and Analysis of Data," Report FAA-RD-74-39-II, U.S. Department of Transportation, Federal Aviation Administration, September, 1975.
5. Steve L.Webster, "Geogrid Reinforced Base Courses for Flexible Pavements for Light Aircraft: Test Section Construction, Behavior Under Traffic, Laboratory Tests, and Design Criteria," Report DOT/FAA/RD-92-25, U.S. Department of Transportation, Federal Aviation Administration, July, 1992.
6. U.S. Army Corps of Engineers, Waterways Experiment Station "Certain Requirements for Flexible Pavement Design for B-29 Airplanes," Waterways Experiment Station, Vicksburg, Mississippi, August, 1945.